Biophysical Chemistry 254 (2019) 106261

Contents lists available at ScienceDirect

Biophysical Chemistry

journal homepage: www.elsevier.com/locate/biophyschem

High pressure response of ^{1}H NMR chemical shifts of purine nucleotides

Claudia E. Munte[a], Matthias Karl[a], Waldemar Kauter[a], Lukas Eberlein[b], Thuy-Vy Pham[a], Markus Beck Erlach[a], Stefan M. Kast[b], Werner Kremer[a], Hans Robert Kalbitzer[a,*]

[a] University of Regensburg, Institute of Biophysics and Physical Biochemistry, Center of Magnetic Resonance in Chemistry and Biomedicine, Universitätsstraße 31, 93053 Regensburg, Germany
[b] TU Dortmund University, Physical Chemistry III, Otto-Hahn-Straße 4a, 44227 Dortmund, Germany

HIGHLIGHTS

- ^{1}H chemical shifts of purine 5′- ribonucleotides at pressures up to 200 MPa.
- The pressure response of the ^{1}H chemical shifts is non-linear.
- The 5′ protons were stereospecifically assigned; errors in literature were corrected.
- The conformational equilibria were studied experimentally.
- Quantum-chemical calculation of AMP fit well to the experiments.

GRAPHICAL ABSTRACT

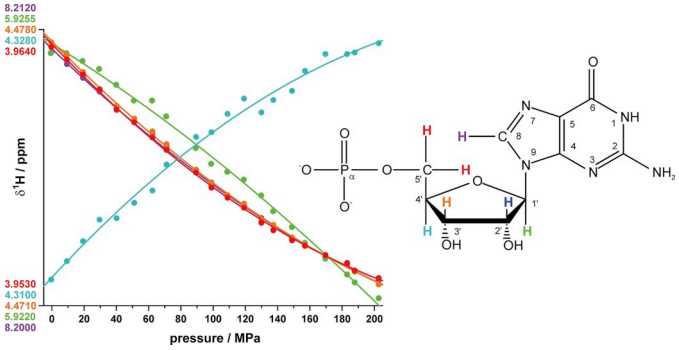

ARTICLE INFO

Keywords:
^{1}H NMR
High pressure NMR spectroscopy
Guanine nucleotide
Adenine nucleotide
AMP

ABSTRACT

The study of the pressure response by NMR spectroscopy provides information on the thermodynamics of conformational equilibria in proteins and nucleic acids. For obtaining a database for expected pressure effects on free nucleotides and nucleotides bound in macromolecular complexes, the pressure response of ^{1}H chemical shifts and *J*-coupling constants of the purine 5′-ribonucleotides AMP, ADP, ATP, GMP, GDP, and GTP were studied in the absence and presence of Mg^{2+}-ions. Experiments are supported by quantum-chemical calculations of populations and chemical shift differences in order to corroborate structural interpretations and to estimate missing data for AMP. The preference of the ribose *S* puckering obtained from the analysis of the experimental *J*-couplings is also confirmed by the calculations. In addition, the pressure response of the non-hydrolysable GTP analogues GppNHp, GppCH_2p, and GTPγS was examined within a pressure range up to 200 MPa. As observed earlier for ^{31}P NMR chemical shifts of these nucleotides the pressure dependence of chemical shifts is clearly non-linear in most cases. In di- and tri-phospho nucleosides, the resonances of the two protons bound to the ribose 5′ carbon are non-equivalent and can be observed separately. The *gg*-rotamer at C4′- C5′ bond is strongly preferred and the downfield shifted resonance can be assigned to the H5″ proton in the nucleotides. In contrast, in adenosine itself the frequencies of the two resonances are interchanged.

Abbreviations: AMP, adenosine-5′-mono-phosphate; ADP, adenosine-5′-di-phosphate; ATP, adenosine-5′-tri-phosphate; GMP, guanosine-5′-mono-phosphate; GDP, guanosine-5′-di-phosphate; GTP, guanosine-5′-tri-phosphate; GTPγS, guanosine-5′-O-(γ-thio)triphosphate; GppNHp, guanosine-5′-(β,γ-imido)triphosphate; GppCH_2p, guanosine-5′-(β,γ-methylene)triphosphate

* Corresponding author.
E-mail address: hans-robert.kalbitzer@ur.de (H.R. Kalbitzer).

https://doi.org/10.1016/j.bpc.2019.106261
Received 3 August 2019; Received in revised form 1 September 2019; Accepted 1 September 2019
Available online 03 September 2019

1. Introduction

High pressure NMR spectroscopy has evolved to an elegant tool to study macromolecular complexes (see e. g. Akasaka and Matsuki [1]) as well as the physicochemical behaviour of small molecules including the solvent itself.

Macromolecules such as proteins and nucleic acids are involved in equilibria of functional states with equilibrium constants which are determined by the difference in their Gibbs free energies ΔG^0. By changing an external physical parameter such as pressure, according to Le Châtelier's principle [2] a state of the system with a lower total volume is preferred. In solution, the trivial result usually is a compression of the molecules of the solvent as well as the solute. More important, also intrinsic equilibria are shifted. Conformers with lower specific molar volumes are preferred that have often also an increased solvation surface (for short overview see e.g. Luong et al. [3]). A well-studied example for such a shift between conformational states is the Ras protein. In ^{15}N HSQC NMR experiments four different states can be observed when analysing ^{15}N and ^{1}H pressure dependent chemical shifts [4]. By analysing the pressure response of ^{31}P NMR chemical shifts at least two of the states can be identified [5]. When adding the information of the pressure response of ^{31}P chemical shifts of model nucleotides [6,7] again 4 states can be characterized from the chemical shift pressure response. Although chemical shift changes are the most easily determined high pressure sensors, the pressure dependence of any other NMR parameter can be used like *J*-couplings [8,9], relaxation times [10] and chemical exchange processes [11,12].

Nucleotides are fundamental molecules of life since they are the building blocks of all genetic material. Nucleic acids determine transcription and translation processes from genes to proteins and have their exclusive functional role as ribozymes, riboswitches and micro RNAs. The monomeric purine units adenosine 5′-triphosphate and guanosine 5′triphosphate are used within the cell to store, transport and supply energy by their phosphoric anhydride bonds. Further, guanine nucleotides determine the “on” and “off” state of an important class of molecular switches, i.e. guanine nucleotide binding proteins (GNBPs). Bound to proteins they can serve as tools to monitor structural transitions of these proteins.

In a first approximation, the chemical shifts of a specific atom in a nucleotide bound to a protein can be separated into two contributions, the chemical shifts of the free nucleotides δ_f and the additional chemical shifts induced directly by binding δ_b. Both δ_f and δ_b are possibly pressure dependent.

For an interpretation of pressure induced chemical shift changes in terms of conformational transitions one has to separate simple compression effects from shifts between different structural states. As a first approximation for simple compression effects on the chemical shifts of amino acids in proteins the pressure response of random-coil model peptides is often taken and the corresponding chemical shift changes are subtracted from the observed chemical shift changes before starting with a thermodynamic analysis [13]. Correspondingly, for the analysis of the pressure response of bound nucleotides the pressure dependence of the free nucleotides themselves can be taken, which reflects both the solvent pressure-induced change of electronic structure [14] as well as conformational population shifts.

The ^{31}P chemical shift response of free guanine and adenine nucleotides and their Mg^{2+}-complexes were already published [6,7]. Here we present the pressure dependent ^{1}H chemical shifts of purine nucleotides recorded under identical experimental conditions as used before for the ^{31}P NMR study.

2. Materials and methods

2.1. NMR samples

$GppCH_2$ was purchased from Jena Bioscience (Germany), all other nucleotides were procured from Sigma-Aldrich (Germany). The samples contained 5 mM 5′-adenine or 5′-guanine nucleotides in buffer A (35 mM tris(hydroxymethyl)aminomethane hydrochloride (Tris-HCl), 0.1 mM 2,2-dimethyl-2-silapentane-5-sulfonate (DSS)), and either 0.5 mM ethylene diamine tetra acetate (EDTA) or 15 mM (nucleoside di- and tri-phosphate samples) and 150 mM (nucleoside mono-phosphate sample) $MgCl_2$, respectively. The pH was adjusted to a value about 2–3 units above the apparent pK_a values of the second deprotonation of the terminal phosphate of the respective nucleotide [15–17] by adding HCl or NaOH and measured with a Hamilton Spintrode attached to a Beckman Coulter pH-meter. It was also controlled in the NMR spectrometer using the pH dependence of chemical shifts of the Tris-signal. The pH values used for the different nucleotides are listed in Table 1. The samples further contained 10% D_2O to obtain a lock signal. For the stereospecific assignment of the 5′ protons samples 10 mM nucleotide have been prepared in 20 mM Tris-d_{11} pH 11.5, 50 mM NaCl, 0.5 mM EDTA-d_{16}, 0.05 mM DSS, 99.8% D_2O.

Table 1
^{1}H chemical shifts δ^0 of purine nucleotides at ambient pressure obtained from the fit of the pressure dependent data.[a]

Atom		H2	H8	H1′	H2′	H3′	H4′	H5′	H5″
Compound	pH	δ_0 [ppm][b]							
ATP	10.5	8.24	8.55	6.13	4.82	4.63	4.39	4.20	4.29
Mg^{2+}.ATP	10.2	8.20	8.50	6.12	4.79	4.57	4.40	4.24	4.29
ADP	10.8	8.23	8.54	6.13	4.76	4.63	4.37	4.18	4.26
Mg^{2+}.ADP	10.6	8.20	8.51	6.12	4.75	4.57	4.38	4.23	4.23
AMP	9.4	8.23	8.62	6.13	4.80	4.50	4.36	3.99	3.99
Mg^{2+}.AMP	9.3	8.20	8.59	6.12	4.78	4.50	4.37	4.00	4.00
Adenosine	11.5	8.16	8.29	5.99	4.77	4.37	4.28	3.91	3.83
GTP	11.5	-[c]	8.09	5.92	4.78	4.60	4.34	4.14	4.26
Mg^{2+}.GTP	9.0	-[c]	8.15	5.94	4.76	4.55	4.36	4.22	4.26
GDP	9.0	-[c]	8.13	5.93	4.75	4.61	4.32	4.16	4.23
Mg^{2+}.GDP	9.0	-[c]	8.16	5.94	4.72	4.56	4.34	4.21	4.21
GMP	9.0	-[c]	8.21	5.93	4.79	4.48	4.31	3.96	3.96
Mg^{2+}.GMP	9.0	-[c]	8.25	5.95	4.74	4.48	4.32	3.99	3.99
GTPγS	10.0	-[c]	8.12	5.92	4.82	4.65	4.35	4.17	4.31
Mg^{2+}.GTPγS	8.5	-[c]	8.17	5.94	4.80	4.57	4.37	4.24	4.30
GppNHp	9.0	-[c]	8.07	5.91	4.73	4.58	4.33	4.15	4.25
Mg^{2+}.GppNHp	11.1	-[c]	8.16	5.93	4.77	4.55	4.36	4.23	4.23
$GppCH_2p$	12.5	-[c]	8.06	5.88	4.71	4.48	4.32	4.13	4.20
Mg^{2+}.$GppCH_2p$	10.0	-[c]	8.24	5.96	4.68	4.52	4.36	4.22	4.22

[a] Data were recorded at 278 K and analyzed as described in method section. The pH was adjusted to be 2 units higher than the pK_a to avoid chemical shift changes by slightly changing pH. The corresponding values are given. Measurements were performed in absence of free $MgCl_2$ (0.5 mM EDTA) and in presence of 15 mM $MgCl_2$ (all nucleotides except AMP, GMP) or 150 mM $MgCl_2$ (AMP, GMP), respectively. Stereospecific assignments see Table 2.

[b] δ_0 is the chemical shift value obtained at ambient pressure at the corresponding pH.

[c] Not existing.

2.2. NMR spectroscopy

Spectra of the high pressure series were recorded with a Bruker Avance-600 spectrometer operating at a ^{1}H frequency of 600.03 MHz equipped with a Prodigy cold probe (Bruker Biospin, Ettlingen). Data for stereo selective assignments were recorded on a Bruker Avance Neo-800 spectrometer operating at 800.20 MHz equipped with a TCI cryoprobe. Data sets were recorded using a homebuilt online-pressure system including a manually operated piston compressor (for details see Beck Erlach et al. [18]). Pressure was transmitted via a high pressure line (High Pressure Equipment Company, Linden, PA, USA) by water to the high pressure ceramic cell (with an outer diameter of 5 mm and an inner diameter of 3 mm) from Daedalus Innovations LLC (Aston. PA. USA). A PET (polyethylene terephthalate) membrane acts as a flexible separator between the pressure fluid and the aqueous sample. To reduce

the volume of the ceramic cell a cylindrical displacement body of polypropylene was used. Temperature was set to 278 K and controlled using the line separation of the methyl and hydroxyl group of external methanol for calibration [19]. Pressure was corrected by using the linear pressure dependence of the Tris-signal in the sample as described by Karl et al. [7].

One dimensional ^{1}H spectra were recorded with a 1D-NOESY pulse sequence (program noesygppr1D) with presaturation of the water signal. For the assignment TOCSY spectra (program mlevphpr.2) [20] with a mixing time of 80 ms were recorded, for the stereospecific assignment T-ROESY spectra (program roesyphpr.2) [21,22] with a mixing time of 200 ms were recorded. All spectra were referenced to DSS used as internal standard. Resonances are designated according to the IUPAC recommendation [23].

2.3. Stereospecific assignment

The stereo-specific assignment of the non-equivalent ribose methylene H5′ and H5″ was performed by analysis of the ^3J(H4′,H5′) and ^3J(H4′,H5″) couplings and of the interatomic distances d(H4′,H5′), d(H4′,H5″), d(H3′,H5′) and d(H3′,H5″). The J-coupling constants were obtained from ^{1}H-1D spectra, the distances were obtained from T-ROESY spectra with a mixing time of 200 ms.

The population P_{gg}, P_{gt} and P_{tg} of the individual rotamers *gg*, *gt* and *tg* (Fig. 1) may be calculated from the generalized Karplus equation from the observed coupling constants ^3J(H4′,H5″) and ^3J(H4′,H5′) using the parameter set for nucleotides and nucleosides that may not be perfectly staggered in solution [24–26]:

$$1.4P_{gg} + 10.5P_{gt} + 3.8P_{tg} = {}^3J(\mathrm{H4'}, \mathrm{H5''}) \quad (1)$$

$$2.3P_{gg} + 2.6P_{gt} + 10.6P_{tg} = {}^3J(\mathrm{H4'}, \mathrm{H5'}) \quad (2)$$

$$P_{gg} + P_{gt} + P_{tg} = 1 \quad (3)$$

The unknown experimental distances were calculated from the cross peak intensities in the T-ROESY spectra assuming the initial slope approximation and a single conformer. A calibration distance of 0.18 nm between the ribose methylene H5′ and H5″ d(H5′,H5″) and 0.29 nm between H1′ and H2′ d(H1′,H2′) was used [27].

Averaged interproton distances $< d >$ were obtained from the distances d_{gg}, d_{gt}, and d_{tg} and the experimental rotamer probabilities P_{gg}, P_{gt} and P_{tg} with

$$< d > = (P_{gg} d_{gg}^{-6} + P_{gt} d_{gt}^{-6} + P_{tg} d_{tg}^{-6})^6 \quad (4)$$

The three rotamers *gg* (ω = −65°), *gt* (ω = 65°) and *tg* (ω = 180°) were built with the program Winmostar (https://winmostar.com/en/index.php) using the two AMP structures with a 3′-*endo* twist (*N*-state) and 2′-*endo* twist (*S*-state) ribose ring puckering that were taken for the chemical shift calculation (see below). The distances in the ribose ring calculated for the *gg*-, *gt*-, and *tg*-rotamers in the *N*-state are, respectively: d(H5″,H4′) 0.245 nm, 0.306 nm, 0.249 nm; d(H5′,H4′) 0.252 nm, 0.251 nm. 0.306 nm; d(H5″,H3′) 0.300 nm, 0.252 nm, 0.370 nm; d(H5′,H3′) 0.370 nm, 0.281 nm and 0.251 nm. In the *S*-state the distances are d(H5″,H4′) 0.242 nm, 0.304 nm, 0.244 nm; d(H5′,H4′) 0.246 nm, 0.252 nm. 0.304 nm; d(H5″,H3′) 0.259 nm, 0.286 nm, 0.372 nm; d(H5′,H3′) 0.372 nm, 0.244 nm and 0.284 nm.

2.4. Sugar pucker conformation from J-couplings

From the values of the NMR coupling constants the sugar pucker conformations *N* and *S* can be calculated according to [28]. As the ribose is expected to be in a conformational equilibrium in nucleosides and their derivatives in solution, the experimental coupling constants J_{exp} will be a population-average of J_N and J_S which is related to their relative populations P_S and P_N = 1- P_S by

$$J_{exp} = P_S J_S + (1 - P_S) J_N \quad (5)$$

Following the IUPAC recommendations [23], in a ribose ring, ^3J(H1′,H2′) ≈ 1 Hz is typical for the *N*-puckered conformation, and ^3J(H1′,H2′) ≈ 7.9 Hz for the *S*-puckered conformation. Using these parameters an estimation of the *S*-conformation to the North ⇌ South equilibrium can be made using the relation

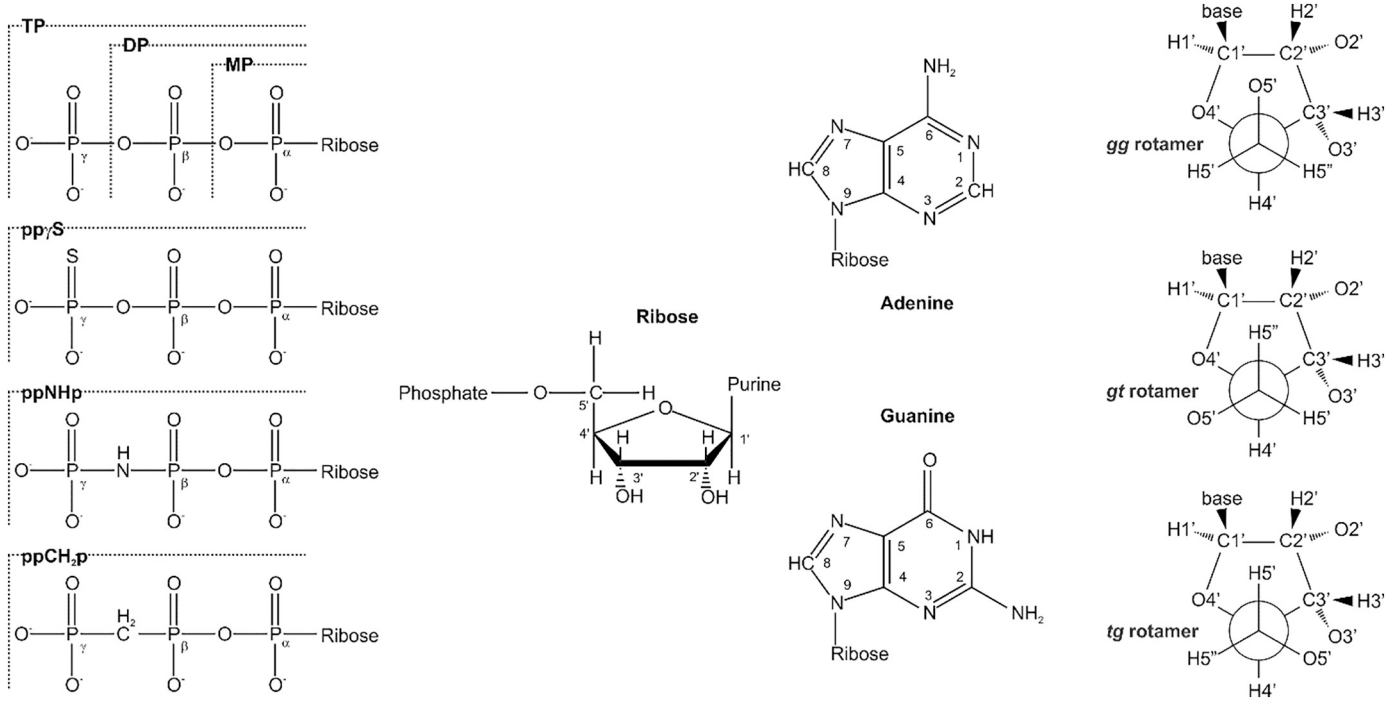

Fig. 1. Structures of different purine nucleotides. The phosphates are labelled with α, β, and γ, in mono-phosphate (MP), di-phosphate (DP), and tri-phosphate (TP) nucleosides. (left) schematic view of the different purine nucleotides. (right) definition of the different rotamers of 5′ protons of ribose. According to IUPAC recommendations H5′ corresponds to the pro-*S* and H5″ to the pro-*R* proton [23].

Table 2
J-couplings and interatomic distances used for stereospecific assignments of H5′ and H5″.[a]

	J-couplings [Hz]					Populations [%]		
	^2J(H5″,H5′)	^3J(H5″,H4′)	^3J(H5′,H4′)	^3J(H5″,Pα)	^3J(H5′,Pα)	P_{gg}	P_{gt}	P_{tg}
Adenosine	12.9	3.4	2.7	-[b]	-[b]	75	21	4
ADP	11.8	2.9	2.9	6.3	4.2	78	15	7
ATP	11.8	2.6	2.7	6.4	4.1	84	12	4
GDP	11.7	3.2	3.3	6.4	4.6	72	17	11
GTP	11.7	2.9	3.0	6.5	4.4	78	14	8
GTPγS	12.0	2.9	3.2	6.3	4.2	76	14	10
GppNHp	11.6	3.1	3.2	6.7	4.8	74	16	10
$GppCH_2p$	11.6	3.3	3.3	6.1	4.7	71	18	11

	Cross peaks [ppm]			
	H5″/H4′	H5′/H4′	H5″/H3′	H5′/H3′
Adenosine	3.83/4.27	3.90/4.27	3.83/4.36	3.90/4.36
ADP	4.25/4.37	4.19/4.37	4.25/4.61	4.19/4.61
ATP	4.29/4.39	4.19/4.39	4.29/4.62	4.19/4.62
GDP	4.21/4.32	4.14/4.32	4.21/4.57	4.14/4.57
GTP	4.26/4.34	4.14/4.34	4.25/4.57	4.15/4.57

	Distances [nm]			
	d(H5″,H4′)	*d*(H5′,H4′)	*d*(H5″,H3′)	*d*(H5′,H3′)
Adenosine	0.25 (0.25/0.25)	0.25 (0.25/0.25)	0.27 (0.29/0.27)	0.31 (0.32/0.30)
ADP	0.24 (0.24/0.25)	0.25 (0.25/0.25)	0.28 (0.29/0.27)	0.31 (0.32/0.31)
ATP	0.23 (0.24/0.25)	0.25 (0.25/0.25)	0.27 (0.29/0.26)	0.31 (0.33/0.32)
GDP	0.25 (0.25/0.25)	0.25 (0.25/0.25)	0.27 (0.29/0.27)	0.30 (0.31/0.30)
GTP	0.23 (0.24/0.25)	0.25 (0.25/0.25)	0.27 (0.29/0.27)	0.32 (0.32/0.31)

[a] d, interatomic experimental and theoretical ^{1}H—^{1}H distances. Experimental distances were obtained from T-ROESY cross peaks assuming the linear slope approximation and a calibration distance of 0.18 nm for *d*(H5″,H5′) and 0.29 for *d*(H1′,H2′). Values in brackets, predicted distances for a *N* (3′-endo) and an *S* (2′-endo) ribose twist when the data base distances for the three rotamers were suitably weighted with the experimental populations from *J*-couplings (Eq. (4) in Materials and Methods).
[b] Not existing.

$$P_S = \frac{^3J(\mathrm{H1'},\mathrm{H2'}) - 1}{6.9} \quad (6)$$

2.5. Analysis of high pressure data

A phenomenological description of the pressure dependence of chemical shifts $\delta(P)$ can be obtained by a Taylor expansion of the pressure dependence as (see e. g. Inoue et al. [29])

$$\delta(P, T_0) = \delta_o + B_1(P - P_0) + B_2(P - P_0)^2 + B_3(P - P_0)^3 + \ldots \quad (7)$$

with δ_0 the chemical shift at pressure P_0 and temperature T_0, B_1, B_2, and B_3 the first, second and third order pressure coefficients at P_0, T_0. In many cases, a fit by a polynomial of second degree is sufficient for a description of the experimental data.

2.6. Calculation of chemical shifts of AMP

The AMP structures were taken from the PDB (https://www.rcsb.org/ligand/AMP) in the *anti-S-gt* conformation and manually rotated to an *anti-S-gg* conformation with O4′-C1′-N9-C4 torsion angle = -150^0 and O-C5′-C4′-O1′ torsion angle = -65^0. *N*-state ribose structures were modified manually from the GDP structure in the PDB (https://www.rcsb.org/ligand/GDP) to an *anti-N-gg* conformer with O4′-C1′-N9-C4 torsion angle = -150^0 and O-C5′-C4′-O1′ torsion angle = -65^0. These structures were optimized at the B3LYP/6–311 + G(d,p) level of theory with the IEFPCM (integral equation formalism polarizable continuum model) solvation approach using the default settings within Gaussian09 [30]. The resulting structures are provided in supplemental Table S1. Single point NMR calculations were done using the EC-RISM (embedded cluster reference interaction site model) solvation theory [31] at the MP2/6–311 + G(d,p) level, using the PSE-2 closure [32] and the GAFF force field 1.4 [33,34] during RISM iterations. This level of theory and all convergence criteria were already successfully applied during the SAMPL blind prediction challenges [35,36]. The solvent susceptibility functions were generated from modified SPC/E water using dielectrically consistent 1D RISM/HNC (hypernetted chain) as in Frach and Kast [37] and Frach et al. [14]. Gauge-invariant atomic orbital (GIAO-)NMR calculations were done using Gaussian 16 [38].

3. Results

3.1. ^{1}H spectra at ambient pressure and spectral assignments

^{1}H NMR assignments of nucleotide resonances are known from literature (see e. g. Kline and Serianni [26]). Since chemical shifts are temperature and buffer dependent they were checked by TOCSY-spectroscopy where necessary. The used nomenclature is shown in Fig. 1. The chemical shifts at ambient pressure δ_0 are summarized in Table 1. In the absence of $MgCl_2$ the two protons bound to C5′ are clearly inequivalent in all studied nucleoside tri-phosphates ATP, GTP, GTPγS, $GppCH_2p$, and GppNHp and the nucleoside di-phosphates ADP and GDP (Supplemental Fig. S1). They are also well-separated in adenosine itself. The largest separation of the two resonances H5′ and H5″ of 0.14 ppm is found for GTPγS, the smallest separation of 0.07 ppm for $GppCH_2p$ and GDP (Table 1, Supplemental Fig. S1). The corresponding downfield respectively upfield shifted resonances in the different nucleotides show rather similar coupling patterns suggesting that the stereo chemical assignment of the two protons can be transferred between the different

nucleotides studied.

In the two mono-phosphate nucleosides AMP and GMP, the two protons bound to C5′ are equivalent with ^{3}J(H5′/H5″,Pα) of 4.4 (pH 9.0) and 4.6 Hz (pH 9.4), respectively. At pH 11.4 these protons become slightly inequivalent in GMP but stay equivalent in AMP. This may be due to the fact that the N-1 atom in GMP gets completely deprotonated at the high pH. The corresponding pK_a-value in guanosine is 9.2 [39]. In addition, the resonance lines of these protons are shifted > 0.2 ppm downfield relative to the lines in ADP, GDP, ATP, and GTP.

In the presence of Mg^{2+}-ions, most resonance lines are somewhat shifted (Supplemental Fig. S1). For adenosine, ADP, ATP, GDP, GTP, GppNHp, GppCH_2p and GTPγS the H5′ and H5″ resonances are still separated, the downfield shifted resonance line is in approximately same position as in the absence of $MgCl_2$ but the distance to the originally upfield shifted resonance is now smaller. This suggests that stereospecific assignments obtained in the absence of $MgCl_2$ can also be transferred to the complexes with Mg^{2+}. In GDP and AMP the H5′ and H5″ lines are not well separated anymore in the presence of $MgCl_2$.

The stereochemical assignment of the H5′ and H5″ resonances was performed on the basis of coupling constants and ROEs. The analysis of the ^{3}J(H5′/H5″,H4′) coupling constants (Table 2) results in the relative frequencies of the three rotamers *gg*, *gt* and *tg* (as defined in Fig. 1) around the C4′-C5′ bond. On the basis of *J*-couplings Eqs. (1) to (3) lead to the conclusion that always the *gg*-conformer is dominant with a predicted population of 75% for adenosine, 78% for ADP and GTP, 84% for ATP, and 72% for GDP. From the intensities of the ROEs between the H5′ and H5″ atoms and the H3′ atom qualitatively a stereospecific assignment can be performed since the H3′ should be closer to H5″ than to H5′ in the *gg*-rotamer (Fig. 2). The experimentally determined, non-uniformly d^{-6} averaged distances in the ribose moieties (Table 2) can be almost perfectly simulated with Eq. (4) from the experimentally determined populations and standard distances estimated for the three rotamers. Since the stronger H3′-ROE is observed for the downfield shifted resonance of the protons bound to C5′ in ATP, ADP, GTP and GDP, this resonance represents the H5″ (pro-*R*) resonance, the resonance at higher field the H5′ (pro-*S*) resonance (Table 2). Surprisingly, the stereospecific assignment of the proton bound to C5′ is interchanged in adenosine, here the pro-*R* resonance is shifted upfield relative to the pro-*S* resonance (Table 2), in line with the stereospecific assignments published earlier for adenosine [26]. The ^{3}J(H5′,Pα) and ^{3}J(H5″,Pα) in the diphospho- and triphospho-nucleosides are not averaged and differ remarkably with a higher value of approximately 6.4 Hz for the coupling to the H5″ and a lower coupling of about 4.3 Hz for the coupling to the H5′ (Table 2). In the mono-nucleotides a single coupling constant of about 4.4 Hz (AMP) and 4.6 Hz (GMP) is detected.

3.2. Glycosidic torsion angle and ribose puckering

The ROESY-spectrum also provides structural information about the positioning of the base relative to the ribose [40]. For ADP, ATP, GDP, and GTP the H8 is closest to H2′ and most distant to H4′ (Table 3). The combination of ROEs is typical for a predominant *anti*-position of the base, although the ROEs are again non-linearly population weighted. In the adenine nucleotides the signal from H2 can also be detected. As to be expected in the *anti*-configuration, it is more distant to the ribose protons.

The ribose moiety of the nucleotides can occur in two main conformations, called the *S* and *N* conformer. The relative populations of the two conformers can be determined from the ^{3}J(H1′,H2′) [28]. The populations were determined as described in Materials and Methods and are listed in Table 4. For all nucleotides investigated here, the *S*-

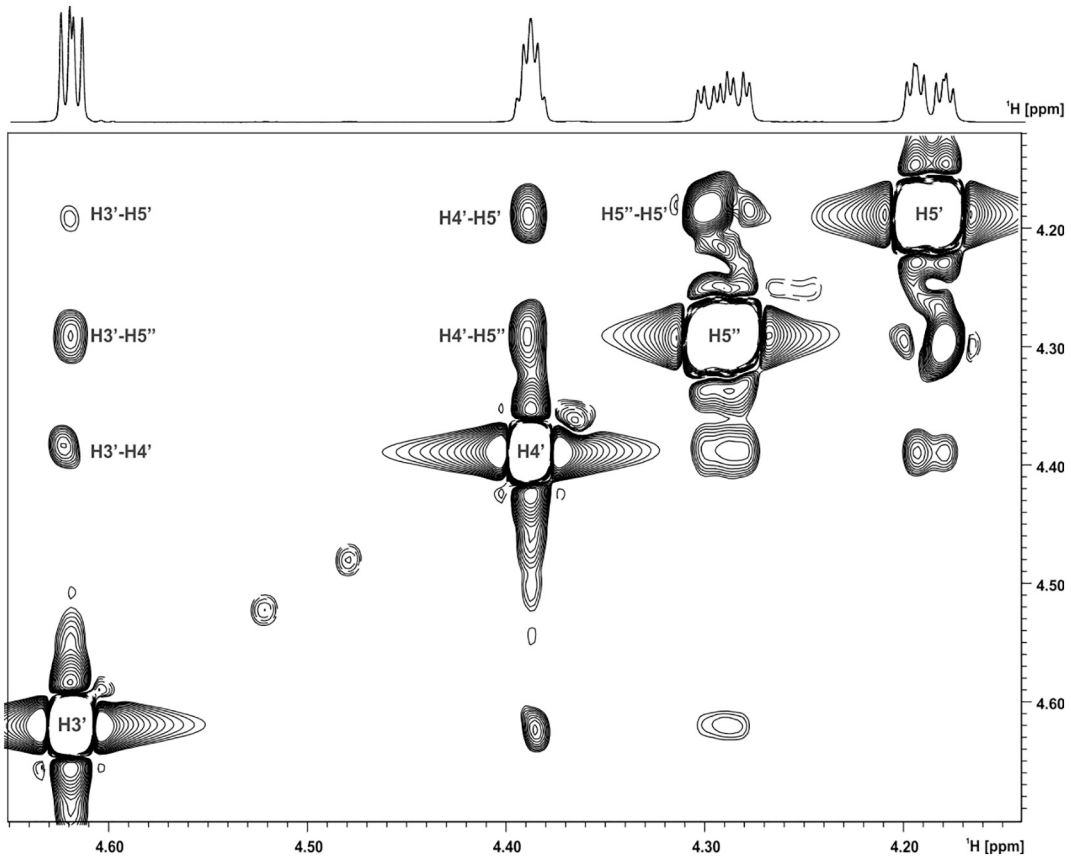

Fig. 2. Part of a T-ROESY-spectrum of GTP. T-ROESY-spectrum recorded at 800.20 MHz and 278 K. The sample contained 10 mM GTP in 20 mM Tris-d11 pH 11.5, 50 mM NaCl, 0.5 mM EDTA-d16, 0.05 mM DSS, 99.8% D_2O.

Table 3
Interatomic distances between purine and ribose atoms.[a]

	Distances [nm]						Populations [%]	
	d(H8,H1′)	*d*(H8,H2′)	*d*(H8,H3′)	*d*(H8,H4′)	*d*(H8,H5″)	*d*(H8,H5′)	P_{syn}	P_{anti}
Adenosine	0.26	0.27	0.33	-[c]	0.40	0.41	40	60
ADP	0.36	0.27	0.33	0.51	0.42	0.40	1	99
ATP	0.35	0.26	0.33	0.43	0.38	0.38	2	98
GDP	0.33	0.25	0.31	0.47	0.41	0.40	6	94
GTP	0.35	0.26	0.34	0.50	0.43	0.41	2	98
syn[b]	0.23	0.33	-[d]	-[d]	-[d]	-[d]		
anti[b]	0.37	0.28	0.43	-[d]	-[d]	-[d]		
	d(H2,H1′)	*d*(H2,H2′)	*d*(H2,H3′)	*d*(H2,H4′)	*d*(H2,H5″)	*d*(H2,H5′)		
Adenosine	0.48	0.44	0.48	-[c]	0.50	0.48		
ADP	0.47	-[c]	-[c]	-[c]	-[c]	-[c]		
ATP	0.45	0.48	0.51	0.61	0.64	0.52		

[a] d, interatomic experimental $^1H—^1H$ distances. Experimental distances were obtained from T-ROESY cross peaks assuming the linear slope approximation and a calibration distance of 0.18 nm for *d*(H5″,H5′) and 0.29 for *d*(H1′,H2′).
[b] Computed proton-proton distances for perfect *syn* and *anti* conformations [40].
[c] No detectable cross-peak.
[d] Not informed.

Table 4
^3J(H1′,H2′) couplings and relative populations of the ribose *N* and *S*- conformers.[a]

	^3J(H1′,H2′)	P_N	P_S
Adenosine	12.9	23	77
AMP	11.8	26	74
ADP	11.8	38	62
ATP	11.7	27	73
GMP	11.7	19	81
GDP	12.0	29	71
GTP	11.6	20	80

[a] Experimental conditions as in Table 1. P_N and P_S populations of the *N* and *S* conformers of the ribose. For details see Materials and Methods.

conformer dominates but both ribose puckerings have significant populations.

3.3. High pressure investigations on adenine nucleotides and their Mg^{2+}-complexes

The ^1H NMR spectra of the three adenine nucleotides AMP, ADP, and ATP were measured at different pressures *P* in the absence and presence of $MgCl_2$ in steps of 10 MPa. Besides the pressure values obtained from the in-line Bourdon manometer the pressure was additionally controlled by the ^1H chemical shifts of the methylene signals of Tris-HCl in the individual samples as described earlier by Karl et al. [7]. Examples of pressure dependent NMR spectra of ADP in the absence and presence of $MgCl_2$ are shown in Fig. 3. The pressure dependencies of the proton chemical shift were fitted with Eq.(7) For all fits a second degree polynomial was sufficient. The pressure response together with the fit curves of the ribose protons are represented in Fig. 4, the corresponding pressure coefficients B_1 and B_2 are given in Tables 5 and 6.

The H8 resonances of the adenine moieties of AMP, ADP, and ATP shift upfield with pressure with similar pressure coefficients. The interaction of the Mg^{2+}-ions with the phosphate groups leads to additional upfield shifts at ambient pressure of 0.03 ppm for AMP and ADP and 0.05 ppm for ATP (Table 1). Note that in AMP with 150 mM $MgCl_2$ a ten times higher ion concentration than for ADP and ATP had to be used since the affinity of AMP for divalent ions is much lower than that for ADP and ATP. With addition of the divalent metal ion the pH slightly drops in all cases. The binding of the metal ion somewhat decreases the pressure induced shifts in the three nucleotides.

In contrast to the H8 resonances for the H2 resonances an increase of pressure leads to a downfield shift. The presence of $MgCl_2$ leads to similar upfield shifts at ambient pressure as observed for the H8 resonances of 0.03 ppm for AMP and ADP and 0.04 ppm for ATP. The presence of the divalent ions results in a somewhat stronger pressure response of the chemical shifts (Fig. 3 and Supplemental Fig. S1). The ratio of $-B_2/B_1$ is related to the local compressibility [13]. For the adenine protons in all three nucleotides it is positive leading to a saturation like behavior.

Almost all proton resonances of the ribose show a significant non-linear pressure dependence with a saturation like behavior (Figs. 3 and 4 and Supplemental Fig. S1). Exceptions are the H1′ resonances of AMP and ATP, the H2′ resonance of Mg^{2+}.AMP, and the H3′ resonance of Mg^{2+}.ADP (Tables 5 and 6). However, since the pressure dependence for these resonances is very small, the parameters have a relatively large error and the sign of the ratio of the pressure coefficients is not well defined.

The pressure response of the chemical shifts of the individual ribose protons depends on the number of phosphate groups bound and on the absence or presence of Mg^{2+}-ions. No simple pattern can be recognized here. The largest shift with pressure of ribose atoms is observed for the H3′ resonance of ADP with a first order pressure coefficient of -0.164 ppm·GPa^{-1} (Table 5).

In general, the binding of Mg^{2+}-ions to the phosphate groups leads to changes of the pressure response of almost all ribose protons. In ADP and ATP, it leads to remarkable changes of the pressure response of the 3′ protons: in the absence of the divalent ions, a strong upfield shift with a strong curvature occurs, in contrast to a weak effect in the presence of the Mg^{2+}-ions. A similar effect can be observed for the 2′ proton of AMP (see Supplemental Fig. S1). The separation of the non-equivalent resonances of the 5′ and 5″ protons of ADP and ATP gets smaller at higher pressures.

In average, a downfield shift (positive B_1) is observed for the H2 of the adenine base and the H4′ of the ribose moiety and an upfield shift (negative B_1) is observed for the adenine H8. No significant shifts are observed for the other atoms (Table 5).

The ^3J coupling constants of the ribose protons do not change significantly with pressure within the limits of error of 0.08 Hz. The same is true for the ^2J coupling constants of the protons bound to C5′ in ADP and ATP and its complexes.

3.4. High pressure investigations on guanine nucleotides and their Mg^{2+}-complexes

The ^1H NMR spectra of the three guanine nucleotides GMP, GDP, and GTP as well as their non-hydrolysable GTP-analogues GppNHp, $GppCH_2p$, and GTPγS were measured at different pressures *P* in the

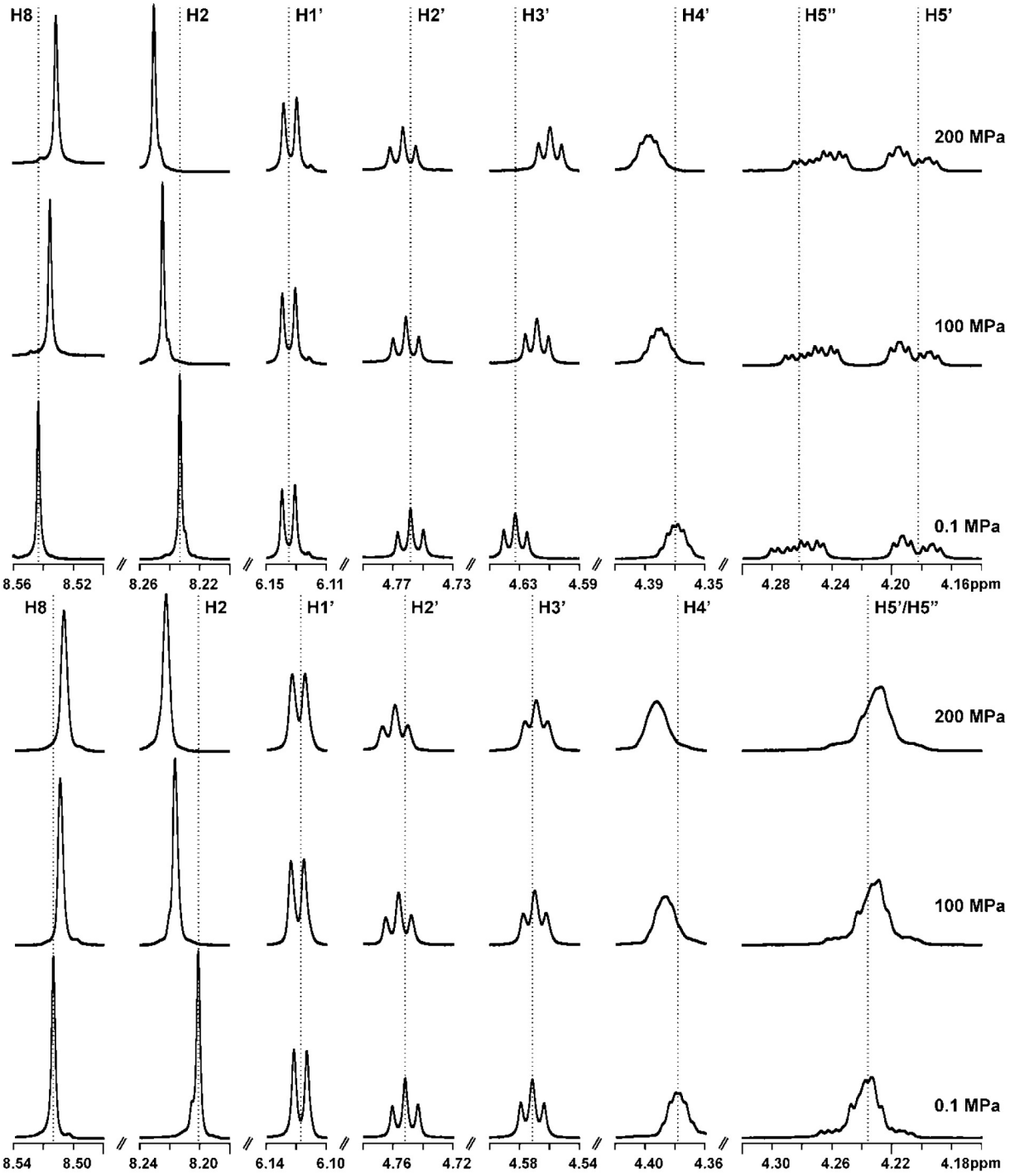

Fig. 3. ^{1}H spectra of ADP at different pressures. The spectra were recorded at a ^{1}H frequency of 600.03 MHz at 278 K at different pressures. The samples contained 5 mM nucleotide in Tris/HCl, 0.1 mM DSS, 10% D_2O. (top) ADP, pH 10.8, 0.5 mM EDTA, (bottom) ADP, pH 10.6, 15 mM $MgCl_2$.

absence and presence of $MgCl_2$ in steps of 10 MPa. Examples of pressure dependent NMR spectra of the non-hydrolysable GTP analogue GppNHp in the absence and presence of $MgCl_2$ are shown in Fig. 5. The pressure dependencies of the proton chemical shift of different guanine nucleotides were fitted with Eq. (7). For all fits a second degree polynomial was sufficient. The pressure response together with the fit curves of the ribose protons are represented in Figs. 6 and 7, the corresponding pressure coefficients B_1 and B_2 are given in Tables 5 and 6.

3.5. Pressure response of guanine nucleotides in the presence and absence of Mg^{2+}-ions

In contrast to adenine nucleotides the H8 resonance of the guanine base does not show a uniform upfield shift with pressure but downfield as well as upfield shifts are observed depending on the number and kind of phosphate groups bound (see Supplemental Fig. S1). The largest first order pressure coefficient of −0.38 ppm/GPa is observed for Mg^{2+}.GppCH_2p (Table 5).

As in the adenine nucleotides most of the proton resonances of the

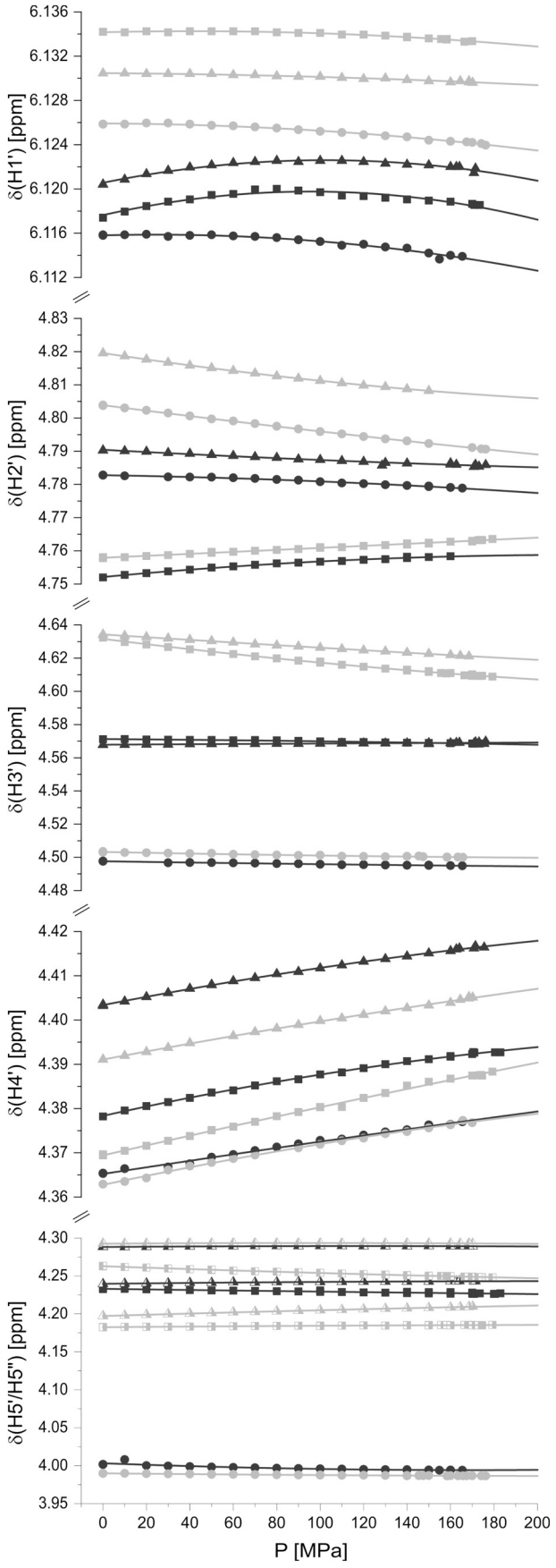

Fig. 4. Pressure dependence of ^{1}H chemical shifts of adenine nucleotides. The pressure dependent ^{1}H chemical shifts δ of AMP, ADP, and ATP in the absence and presence of $MgCl_2$. Experimental conditions see Table 1. (●) AMP, (●) Mg^{2+}.AMP, (■) ADP, (■) Mg^{2+}.ADP, (▲) ATP, (▲) Mg^{2+}.ATP. In case of the non-equivalent 5′ and 5″ protons, the 5″ protons are presented by the corresponding hollow left-filled symbols (◧, ◧, ◭, ◭), while the 5′ protons are represented by right-filled symbols (◨, ◨, ◭, ◭).

ribose show a significant non-linear pressure dependence with a saturation like behavior (Figs. 5, 6, 7 and Supplemental Fig. S1).

The pressure response of the chemical shifts of the individual ribose protons also depends on the number of phosphate groups bound and on the absence or presence of Mg^{2+}-ions. No simple pattern can be recognized here. The largest shift with pressure is observed for the H4′ resonance of $GppCH_2p$ with a first order pressure coefficient of 0.19 ppm/GPa. In general, the binding of Mg^{2+}-ions to the phosphate groups leads to changes of the pressure response of almost all ribose protons. Quite often the direction of the pressure response is inverted in the absence and presence of divalent ions. The non-equivalent resonances of the 5′ and 5″ protons of GDP and the GTP analogs get stronger separated at higher pressures.

In the average, a downfield shift (positive B_1) is observed for the H4′ of the ribose moiety. No significant (within the limits of error) shifts are observed for the other atoms (Table 5).

The ^{3}J coupling constants of the ribose protons do not change significantly with pressure within the limits of error of 0.08 Hz. The same is true for the ^{2}J coupling constants of the protons bound to C5′ in GDP and as well as in GTP and its analogs and its Mg^{2+}-complexes.

3.6. Quantum-chemical calculation of chemical shifts of AMP

GIAO-NMR yielded the isotropic chemical shielding constants of all atoms (Table 7). These shielding constants and a suitable reference shielding constant are used for the calculation of isotropic NMR chemical shifts. The populations of the different conformations were calculated using Boltzmann statistics according to the free energy expression derived in Tielker et al. [36]. The population-weighted chemical shielding constants were calculated by multiplying the population of the respective conformation with the corresponding shielding constants and summing up over all conformations. In addition to the chemical shifts also the relative populations of the ribose *N* and *S* ring puckering, the free enthalpy difference between the two states, and the difference of the partial molar volumes could be predicted.

4. Discussion

4.1. Stereochemical assignment of the ribose H5′ and H5″ resonances

In most of the nucleotides studied here, the two protons bound to the ribose C5′ are not equivalent and can be observed separately (Table 1). This is also true for adenosine itself. By selective deuteration of the pro-*S* proton bound to the ribose C5′ in adenosine, guanosine, cytidine, and uridine it was shown that the downfield shifted proton resonance corresponds to the pro-*S* proton (in our nomenclature to H5′) in all four nucleosides [26]. The *gg*-rotamer is always prevailing in these nucleosides.

In contrast, in all nucleotides studied here, where the two protons are well separated in the spectra, the H5′ resonance is always shifted upfield relative to the H5″ resonance. The assignment was performed on the basis of the ^{3}J-coupling constants between H4′ and H5′ and H5″ (Table 2) and ROEs in the ribose. The analysis of the ^{3}J-coupling constants predict a prevalence of the *gg*-rotamer with relative populations of > 71%. In principle, from this analysis also the stereochemical assignment can be derived when the ^{3}J-coupling constants derived for the different rotamers for the nucleosides can be transferred to our

Table 5
^{1}H pressure coefficients B_1 of purine nucleotides obtained from the fit of the pressure dependent data.[a]

Atom		H2	H8	H1′	H2′	H3′	H4′	H5′	H5″
Compound	pH	B_1 [ppm/GPa][b]							
ATP	10.5	0.1342	−0.113	−0.0014	−0.099	−0.083	0.092	0.083	0.019
Mg^{2+}.ATP	10.2	0.206	−0.054	0.040	−0.035	0.007	0.096	0.032	0.021
ADP	10.8	0.134	−0.090	0.0046	0.029	−0.164	0.113	0.023	−0.100
Mg^{2+}.ADP	10.6	0.204	−0.054	0.045	0.061	−0.010	0.109	−0.038	−0.038
AMP	9.4	0.118	−0.131	−0.0010	−0.084	−0.026	0.104	−0.029	−0.029
Mg^{2+}.AMP	9.3	0.153	−0.122	0.005	−0.011	−0.019	0.075	−0.11	−0.11
Mean[c]		0.158	−0.094	0.015	−0.023	−0.049	0.098	−0.006	−0.039
		(0.038)	(0.034)	(0.021)	(0.062)	(0.064)	(0.014)	(0.066)	(0.055)
GTP	11.5	-[d]	0.037	−0.038	−0.036	−0.076	0.133	0.062	0.027
Mg^{2+}.GTP	9.0	-[d]	−0.051	0.012	−0.020	0.016	0.107	−0.060	0.009
GDP	9.0	-[d]	−0.0085	0.0014	0.004	−0.141	0.125	−0.068	−0.079
Mg^{2+}.GDP	9.0	-[d]	−0.074	−0.002	0.062	−0.004	0.104	−0.079	−0.079
GMP	9.0	-[d]	−0.068	−0.0127	−0.117	−0.0385	0.113	−0.068	−0.068
Mg^{2+}.GMP	9.0	-[d]	−0.213	−0.0576	0.017	−0.0343	0.083	−0.112	−0.112
GTPγS	10.0	-[d]	0.003	−0.024	−0.105	−0.088	0.113	0.014	0.032
Mg^{2+}.GTPγS	8.5	-[d]	−0.021	−0.001	−0.029	0.029	0.093	−0.048	0.010
GppNHp	9.0	-[d]	0.0658	−0.0140	0.013	−0.006	0.137	0.023	0.043
Mg^{2+}.GppNHp	11.1	-[d]	−0.057	0.017	−0.036	−0.004	0.100	−0.001	−0.001
$GppCH_2p$	12.5	-[d]	0.071	0.066	0.091	0.176	0.191	0.002	0.068
Mg^{2+}.$GppCH_2p$	10.0	-[d]	−0.378	−0.040	0.103	0.010	0.095	−0.027	−0.027
Mean[c]		-[d]	−0.06	−0.008	−0.004	−0.013	0.116	−0.030	−0.015
			(0.13)	(0.032)	(0.068)	(0.077)	(0.029)	(0.051)	(0.057)

[a] Data were recorded at 278 K and analyzed as described in method section. For experimental details, see Table 1.
[b] B_1 is the first order pressure coefficients value obtained at ambient pressure at the corresponding pH.
[c] Mean of the B_1- values of adenine and guanine nucleotides, respectively. Values in brackets represent the standard deviation.
[d] Not existing.

nucleotides [24–26]. For corroborating these assignment ROEs were determined allowing the determination of interatomic distances to H5′ and H5″ in ribose. Qualitatively, the ROE between H3′ and H5″ decides about the assignment. The distances *d*(H5′,H3′) and *d*(H5″,H3′) for the *gg*-rotamer in the *N*-state should be 0.370 and 0.300 nm, respectively; in the *S*-state these distances should be 0.372 and 0.259 nm, respectively (see Materials and Methods). The stronger ROE experimentally observed for the H5″-H3′ contact qualitatively confirms the assignment of the H5′ and H5″ given in Fig. 2 and Table 2. In the ROESY-spectra the ROEs including these protons should be averaged. Using the relative populations of the rotamers at the C5′-group determined from the *J*-couplings, a somewhat better agreement is obtained between the

Table 6
^{1}H pressure coefficients B_2 of purine nucleotides obtained from the fit of the pressure dependent data.[a]

Atom		H2	H8	H1′	H2′	H3′	H4′	H5′	H5″
Compound	pH	B_2 [ppm/GPa^2][b]							
ATP	10.5	−0.220	0.168	−0.020	0.151	0.032	−0.06	−0.07	−0.102
Mg^{2+}.ATP	10.2	−0.47	0.05	−0.19	0.04	0.00	−0.115	−0.07	−0.09
ADP	10.8	−0.21	0.147	−0.055	0.006	0.21	−0.04	−0.04	0.10
Mg^{2+}.ADP	10.6	−0.48	0.08	−0.23	−0.14	−0.04	−0.16	0.02	0.02
AMP	9.4	−0.20	0.19	−0.056	0.048	0.04	−0.12	0.056	0.056
Mg^{2+}.AMP	9.3	−0.36	0.14	−0.11	−0.08	0.02	−0.02	0.3	0.3
Mean[c]		−0.32	0.130	−0.111	0.00	0.044	−0.086	0.03	0.05
		(0.13)	(0.052)	(0.085)	(0.10)	(0.086)	(0.051)	(0.15)	(0.15)
GTP	11.5	-[d]	−0.011	0.063	0.056	0.10	−0.20	−0.09	−0.064
Mg^{2+}.GTP	9.0	-[d]	0.117	−0.08	0.03	−0.025	−0.16	0.15	−0.01
GDP	9.0	-[d]	0.019	−0.044	−0.024	0.18	−0.16	0.107	0.105
Mg^{2+}.GDP	9.0	-[d]	0.10	−0.08	−0.12	−0.004	−0.14	0.07	0.07
GMP	9.0	-[d]	0.087	−0.018	0.15	0.052	−0.19	0.106	0.106
Mg^{2+}.GMP	9.0	-[d]	0.36	0.047	−0.087	0.051	−0.08	0.14	0.14
GTPγS	10.0	-[d]	0.02	0.005	0.17	0.04	−0.09	0.04	−0.09
Mg^{2+}.GTPγS	8.5	-[d]	0.061	−0.059	0.04	0.02	−0.064	0.05	0.01
GppNHp	9.0	-[d]	−0.038	0.007	−0.036	−0.041	−0.19	0.018	−0.081
Mg^{2+}.GppNHp	11.1	-[d]	0.099	−0.07	−0.02	0.004	−0.14	−0.09	−0.09
$GppCH_2p$	12.5	-[d]	−0.10	−0.200	−0.26	−0.48	−0.39	0.03	−0.20
Mg^{2+}.$GppCH_2p$	10.0	-[d]	0.70	0.02	−0.19	−0.02	−0.20	0.01	0.01
Mean[c]		-[d]	0.12	−0.034	−0.02	−0.01	−0.166	0.044	−0.01
			(0.22)	(0.071)	(0.13)	(0.16)	(0.086)	(0.076)	(0.10)

[a] Data were recorded at 278 K and analyzed as described in method section. For experimental details, see Table 1.
[b] B_2 is the second order pressure coefficients value obtained at ambient pressure at the corresponding pH.
[c] Mean of the B_2- values of adenine and guanine nucleotides, respectively. Values in brackets represent the standard deviation.
[d] Not existing.

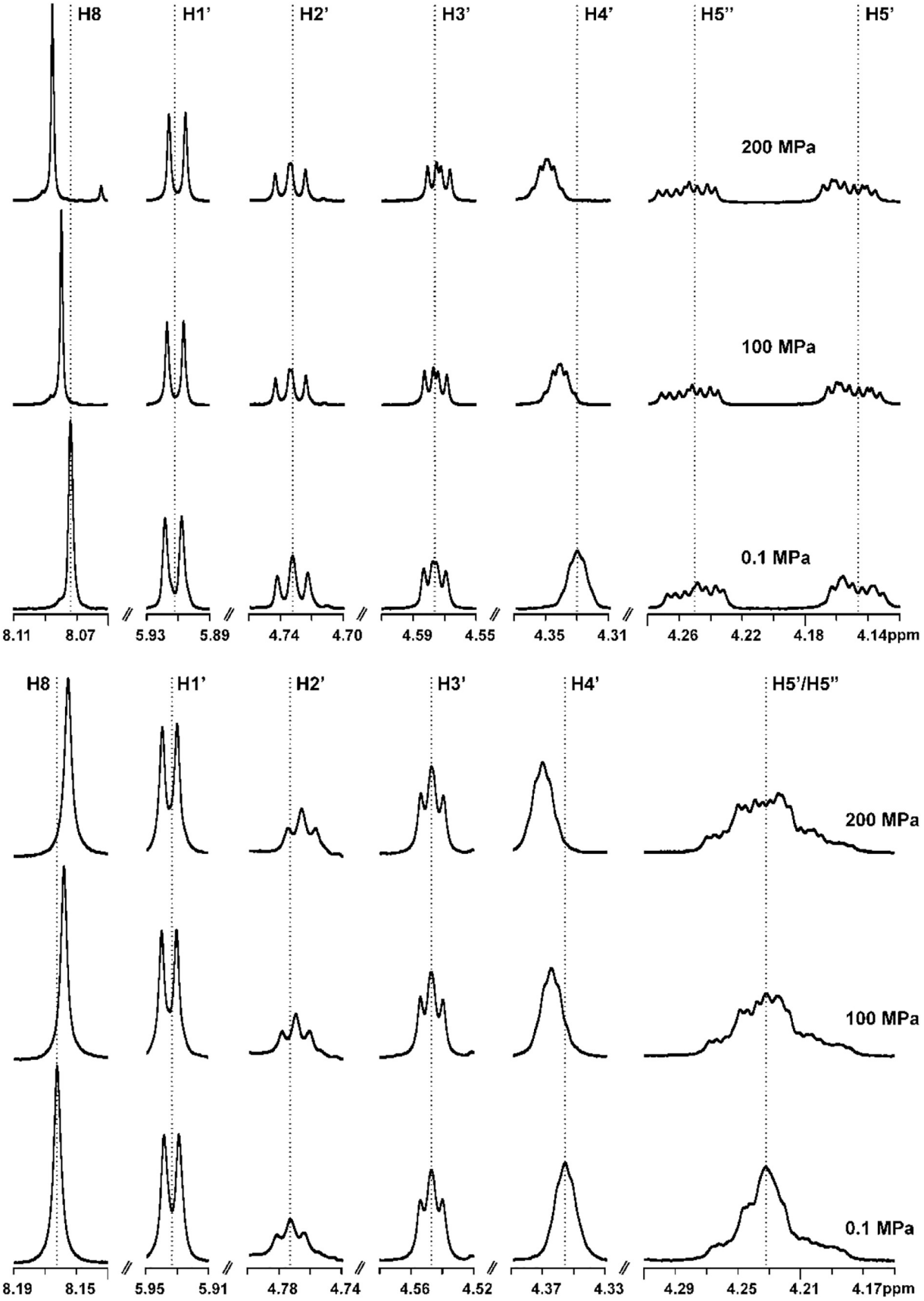

Fig. 5. ^{1}H spectra of GppNHp at different pressures. The spectra were recorded at a ^{1}H frequency of 600.03 MHz at 278 K at different pressures. The samples contained 5 mM nucleotide in Tris/HCl, 0.1 mM DSS, 10% D_2O. (top) GppNHp, pH 9.0, 0.5 mM EDTA, (bottom) GppNHp, pH 11.1, 15 mM $MgCl_2$.

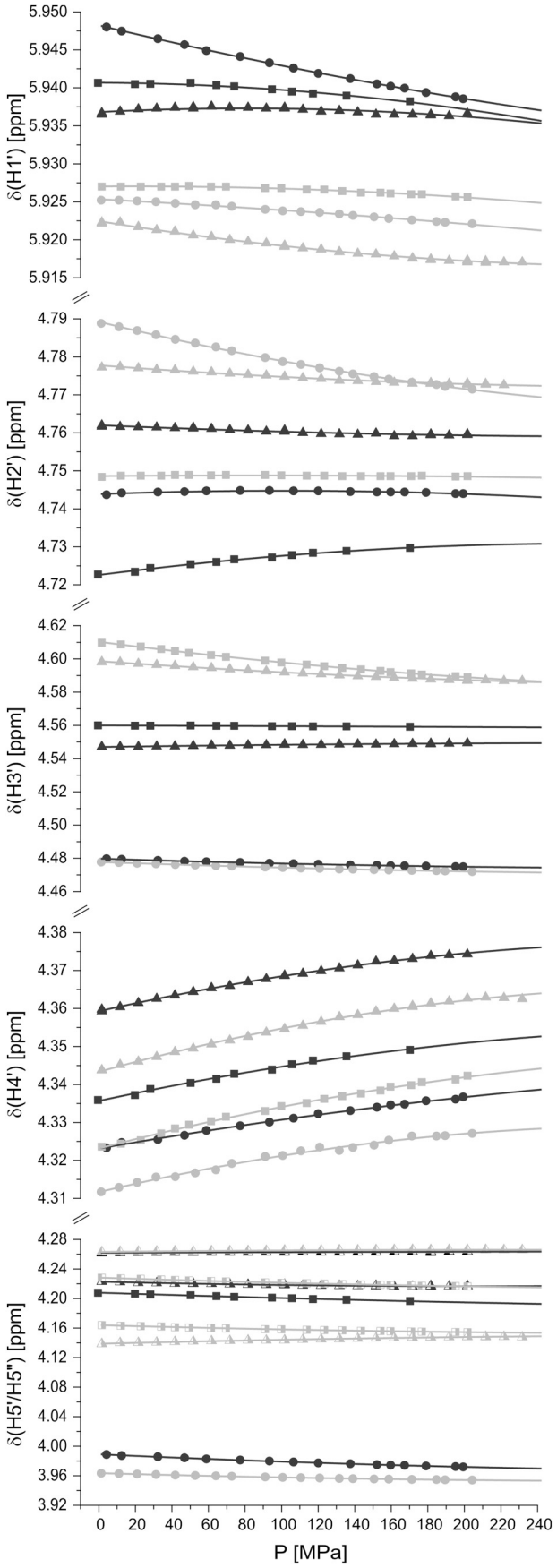

Fig. 6. Pressure dependence of ^{1}H chemical shifts of natural guanine nucleotides. The pressure dependent ^{1}H chemical shifts δ of free GMP, GDP, and GTP in the absence and presence of $MgCl_2$. Experimental conditions see Table 1. (●) GMP, (●) Mg^{2+}.GMP, (■) GDP, (■) Mg^{2+}.GDP, (▲) GTP, (▲) Mg^{2+}.GTP. In case of the non-equivalent 5′ and 5″ protons, the 5″ protons are presented by the corresponding hollow left-filled symbols (◧, ◧, ◭, ◭), while the 5′ protons are represented by right-filled symbols (◨, ◨, ◭,◭).

observed and the expected ROEs of a 2′-*endo* twist (*S*-state) ribose ring puckering (Table 2). Since the adenosine data were recorded by Kline and Serianni [26] at a different temperature and a not defined pH, we repeated the experiments under our conditions. Our experiments (Table 2) confirmed their assignment. Interestingly, the introduction of two or three phosphate groups inverses the order of the H5′ and H5″ resonances in the spectra. Note that sometimes in the literature a different (wrong) stereochemical assignment is reported for ADP, ATP, GDP, and GTP as e. g. by Son and Chachaty [41]. In the absence of Mg^{2+}-ions the two protons bound to the C5′ are well separated for all di- and tri-phospho nucleosides, only in AMP and GMP the resonances cannot be separated (Table 1). From their coupling patterns they are equivalent (Table 1, Supplemental Fig. S1). This equivalence disappears in the presence of $MgCl_2$.

For the other nucleotides the addition of $MgCl_2$ leads to a decrease of the line separation. As a rule the resonance position of H5″ is largely unaffected but the H5′ resonance is shifted downfield (Table 1). As a consequence in some cases the two resonances strongly overlap and cannot be distinguished anymore.

4.2. Theoretical AMP populations and chemical shifts

Experimental results show a preference for the *gg*-rotamer and the *anti*-conformation in Adenosine, ADP and ATP, whereas AMP populations cannot be resolved experimentally due to the indistinguishability of H5′ and H5″ chemical shifts. The preferred conformations, *anti-gg*, are apparently stabilized by increasing the length of the phosphate chain (Tables 2 and 3), yet uncertainty persists for the relative importance of *anti-gg* sub-conformations characterized by the equally possible *N* and *S* states. Calculated populations show a slight preference for the *S*-state (Table 7). Experimental data for this equilibrium are not available for AMP but only for adenosine, ADP, GDP, ATP and GTP (Table 2) and thus a direct comparison between theory and experiment for AMP is not possible. In these compounds, also a weak preference for the *S*-state from experimental ROEs is observed. This is also consistent with the experimental data. The analysis of the ^{3}J(H1′,H2′) predicts that the *S* states are preferred. Here, the population of the two ribose ring puckering states P_N and P_S could be determined for all purine nucleotides including AMP. A relative population P_S of 74% was estimated. The theory predicts a value of 83%, very close to the NMR estimate. In addition, the energetic differences resulting in these populations are in the order of only 1 kcal mol^{-1} and therefore within the expected range of errors [35,36], even without considering further uncertainty concerning ribose-OH conformations.

NMR calculations were further used for investigating the similarity of H5′ and H5″ chemical shifts in AMP, which is possible by simply computing the difference of shielding constants (taking into account that this quantity enters the chemical shift expression with a negative sign). The experimental chemical shifts of the base protons H2 and H8 show an upfield shift of the H2 resonance relative to H8 in the range of 0.13 ppm (adenosine, Table 1) to 0.39 ppm (AMP). This is in agreement with the calculations (0.93 ppm for AMP). This benchmark therefore corroborates the computational setup as the calculated chemical shifts are reasonable even when using only two conformations, and can be used for the investigations of the experimentally unresolved H5′ and H5″ difference for AMP which is 3.99 ppm (Table 1). In contrast, adenosine shows an upfield shift of the H5″ compared to the H5′ resonance

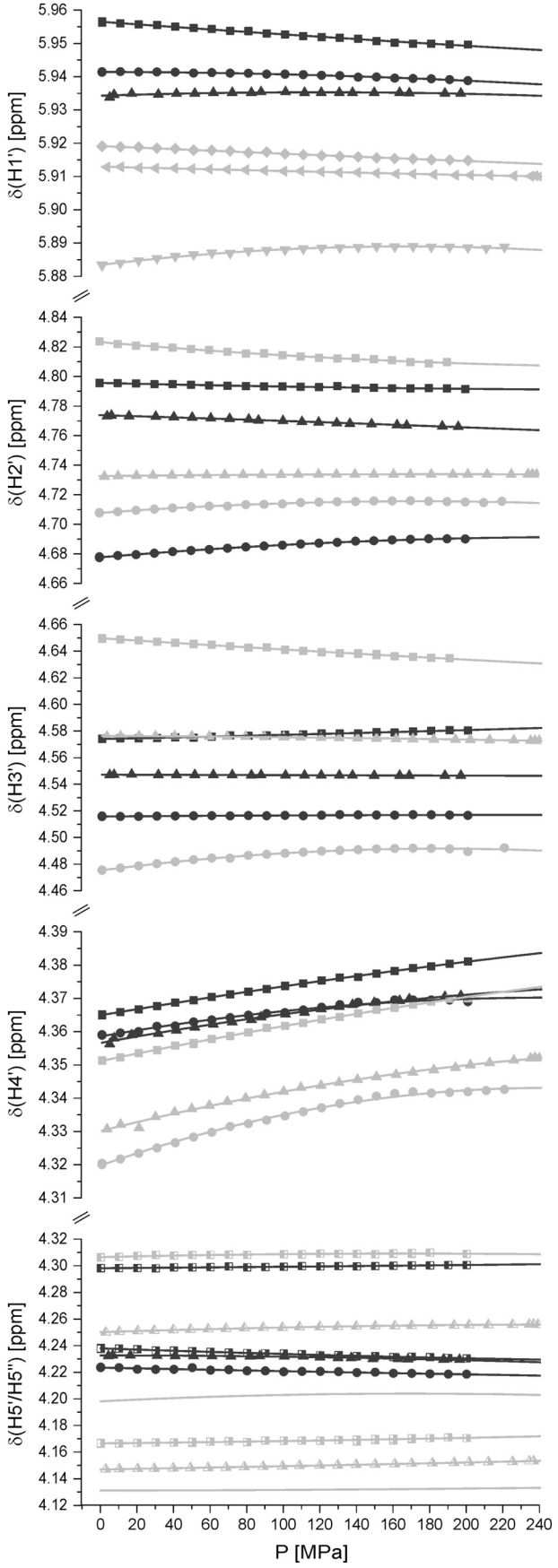

Fig. 7. *Pressure dependence of ^{1}H chemical shifts of guanine nucleotide analogs.* The pressure dependent ^{1}H chemical shifts δ of free GppCH$_2$p, GTPγS, and GppNHp in the absence and presence of $MgCl_2$. Experimental conditions see Table 1. (●) GppCH$_2$p, (●) Mg^{2+}.GppCH$_2$p, (■) GTPγS, (■) Mg^{2+}.GTPγS, (▲) GppNHp, (▲) Mg^{2+}.GppNHp. In case of the non-equivalent 5′ and 5″ protons, the 5″ protons are presented by the corresponding hollow left-filled symbols (◧, ◧, ◭, ◭), while the 5′ protons are represented by right-filled symbols (◨, ◨, ◭,◭).

Table 7
Theoretical data for two AMP conformations.[a]

Structure	*Anti-S-gg*	*Anti-N-gg*	Average	δ
x_{conf}	0.833	0.167	–	
σ^0 H2	23.373	23.406	23.379	8.521
σ^0 H8	22.473	22.344	22.451	9.340
σ^0 H1′	25.380	25.446	25.391	6.508
σ^0 H2′	26.552	27.575	26.723	5.177
σ^0 H3′	27.322	26.924	27.256	4.644
σ^0 H4′	27.205	27.440	27.244	4.656
σ^0 H5′	27.818	27.477	27.761	4.139
σ^0 H5″	27.948	27.748	27.914	3.986
E_{intra}	−4,011,251.96	4,011,185.60	–	
μ_{ex}	−1262.28	−1324.70	–	
$\mu_{ex,corr}$	−1212.71	1275.13	–	
ΔG_{rel}	0	3.98		
$P_{N,S}$	0.83	0.17		
PMV	183.854	183.807	–	

[a] x_{conf}, populations of the conformers; σ^0, ^{1}H chemical shielding constants at ambient pressure (in ppm); E_{intra}, intramolecular energy (in kJ mol^{-1}); μ_{ex}, excess chemical potential without and with ($\mu_{ex,corr}$) partial molar volume correction (in kJ mol^{-1}); $\Delta G_{rel} = \mu_{ex,corr} + E_{intra} - (\mu_{ex,corr} + E_{intra})_{min}$, total free energy relative to the minimum free energy structure *anti-S-gg*; PMV, partial molar volume (in Å^3). $P_{N,S}$ are the relative of the *N* and *S* state of the ribose. δ contains the calculated, population weighted, isotropic chemical shifts corresponding to the respective chemical shielding constants. Shifts are relative to DSS using a reference chemical shielding constant of 31.8997 ppm [54].

(−0.08 ppm) while a downfield shift of the 5″ resonance in ADP (+0.08 ppm) and ATP (+0.09 ppm) is observed. The calculated, population-averaged shielding constants for 5′ and 5″ are inequivalent for AMP and, similar to adenosine, we find an upfield shift of the 5″ resonance (−0.15 ppm), making AMP more "adenosine-like". The absolute value is slightly larger than for ADP and ATP, which altogether means that other factors than internal rotation should play a role for the apparent indistinguishability. A possible explanation could be the chemical shift anisotropy related to phosphorus, which may lead to a stronger downfield shift of the H5″ than the H5′ resonance when the number of neighboring phosphate groups is increased, and which is not captured by the calculation of isotropic shielding constants.

4.3. ^{31}P-^{1}H *J-couplings and conformational equilibria*

The ^3J(H5′,Pα) and ^3J(H5″,Pα) are not identical but differ significantly with the larger coupling constant observed for H5″. This means that the position of the α-phosphorus has a preference relative to the C5′ protons. The effect of Mg^{2+}-ions on these dynamics is difficult to judge since the resonance lines of the two C5′ protons are less separated here and in addition, Mg^{2+}-binding to the Pα-group will change the electronic polarization and thus may change the coupling constants.

The values of the *J*-couplings obtained here are similar to the values reported by Son and Chachaty [41] for ADP (6.5 Hz, 5.0 Hz), ATP (6.5 Hz, 4.9 Hz), GDP (6.5 Hz, 5.5 Hz), and GTP (6.2 Hz, 5.3 Hz) but the second coupling constant is significantly smaller in our case (Table 2). More important, the stereochemical assignment is different in our case which would also change the expected orientation of the phosphate

group. This is probably due to the higher magnetic field we used allowing a better separation of the H5′ and H5″ resonance. The ^3J(H5′,Pα) and ^3J(H5″,Pα) coupling constants are known to be strongly dependent on the torsional angle β around the O5′-C5′ bond [42,43]. The conformer populations obtained using the Karplus parameters from Blackburn et al. [44] would correspond to a preferred *g′g′*-configuration (75% for ADP, ATP and GTPγS; 69% for GppNHp; 73% for GppCH$_2$p). This has been also predicted for the mononucleotides by Davies and Danyluk [43] with a probability > 72% for the *g′g′*-rotamer (ideally β = 180 °).

4.4. Pressure dependent changes of pH and metal affinity

In principle, all chemical shifts of the nucleotides are pH dependent. As already done in the studies of the ^{31}P NMR chemical shifts [6,7] we selected pH values that are about 2 to 3 units higher than the pK_a-values of the terminal phosphate groups. Changes of the pH with pressure can be estimated from the chemical shifts of the Tris methylene protons. The same samples were used in the present study that were also used in the two ^{31}P studies. By observing the chemical shift of the Tris methylene protons, the pH-changes with pressure can be controlled. In all measurements the Tris signal shows a very small upfield shift from ambient pressure to 200 MPa which is < −0.006 ppm at pH 9.3 and − 0.0012 ppm at pH 10.7. It has been concluded that a slight increase of the pH smaller than 0.2 was possible in some samples. Since we are far away from the respective pK_a-values, the pressure dependence of chemical shifts of the nucleotides should be neglectable.

Since pressure usually leads to an increased dissociation of complexes, the affinity of Mg^{2+} to the nucleotides could decrease and therefore lead to additional shift changes. In the ^{31}P NMR studies on purine nucleotides a significant release of ions could not be observed in the pressure dependent phosphorus spectra recorded under our experimental conditions [6,7]. A release of the metal ion should lead to a chemical shift that, at high pressure, are closer to the chemical shift of the free nucleotide. In the extreme case the chemical shift at high pressure should correspond to the value in the free nucleotide. Although in some cases the difference of chemical shifts in the presence and absence of $MgCl_2$ becomes smaller, the effect is quite small. It is also not stronger in AMP or GMP that have the lowest affinity for divalent ions. In summary, the observed chemical shift values at high pressure are most probably not significantly influenced by the release of divalent ions by pressure.

4.5. Factors determining the chemical shift changes with pressure

The pressure response of the observed ^{1}H chemical shifts may be due to many different factors: It may be due to (1) pressure induced changes of the water structure and its interaction with the nucleotides. This interaction may also lead to (2) electric field effects on polarizable group and bond polarization. In addition, (3) the structural ensemble may change with pressure and hence structure dependent contributions to the chemical shifts or (4) a possible aggregation of the nucleotides at high nucleotide concentration influencing the structural equilibria and causing intermolecular chemical shift changes may be modified by pressure.

If there is a common reason such as a shift of a conformational equilibrium for the pressure dependent shift changes, in a first approximation it could lead to correlated chemical shift changes. We have analyzed the correlations between chemical shifts, B_1, and B_2 values for all observed hydrogen atoms of the adenosine and guanine nucleotides in the absence and presence of $MgCl_2$ (Figs. 8 and 9). It turned out, that the B_1 and B_2 coefficients are strongly negative correlated for all base and ribose atoms (except H4′ from adenine nucleotides). Surprisingly also a correlation coefficient > 0.80 is observed between the chemical shifts at ambient pressure and both the first (negative correlation) and second (positive correlation) order pressure coefficients for the base atoms and the ribose H2′. Interestingly no correlations can be found involving H1′ and H2′ and the rest of the ribose atoms neither for the adenine nor for the guanosine nucleotides. In addition, some long range effects are observed for the shifts as well as for the pressure coefficients between the H8 and the ribose atoms H3′, H4′, H5′ and H5″, especially for the guanine nucleotides, indicating that a similar physical cause is responsible for these shifts.

Another interesting correlation is found for the base atom H2 that is not present in guanine. Here, strong effects involving the shift, the B_1 and the B_2 values of adenine H2 and ribose H1′ are clearly present, indicating that their pressure dependent shift changes are directly coupled.

These correlations would be in line with a generalized change of conformation equilibria.

4.6. Concentration dependent chemical shift changes

Nucleotides are known to form dimers and higher aggregates at high nucleotide concentrations. At 1 M concentration and neutral pH about 45% of AMP should form a stacked dimer [52,53]. Pressure is known to influence binding equilibria. Usually a depolymerisation is observed. A shift of the monomer-dimer equilibrium could be responsible for the chemical shift changes with pressure where the observed chemical shifts could be the population averaged chemical shifts of the stacked dimers in fast exchange on the NMR time scale with the monomers. However, in our high pressure NMR experiments we had a significantly lower nucleotide concentration of 5 mM than used in earlier studies. In this concentration range, dimerization should probably be neglectable. As a test we diluted samples by a factor of 10 but could only find very small chemical shift changes of the base and ribose resonances that could not explain our pressure induced shifts (data not shown). When aggregation/disaggregation would be a dominant factor, all resonances should be affected by the shift of the equilibrium in a correlated way: the expected dissagregation with pressure would correspond to the dilution caused shift changes, aggregation to the opposite. However, the direction of the pressure dependent chemical shift changes was not correlated with the observed dilution induced chemical shift changes, the shift changes of a part of the resonances has the same sign as the pressure effects, another part the opposite sign. The same effect can be observed when looking at published data, e. g. the AMP-chemical shifts published in [52]. These data indicate, that a shift of the monomer-dimer equilibrium is not the main factor responsible for the pressure induced shifts.

4.7. Similarity of the ratio of B_2/B_1

The chemical shift dependence on pressure varies from atom to atom and from nucleotide to nucleotide. Up- and downfield shifts of different magnitudes occur (Tables 1, 5, 6; Figs. 4 and 6). However, the shape of the pressure response could be similar, that is the ratio of the Taylor coefficients B_1 and B_2 in our approximation could be similar. Such a behaviour would be expected when the same physical process dominantly determines the pressure response. We have plotted B_2 as a function of B_1 for all resonances in the nucleotides studied (Fig. 10). Indeed, a rather good correlation is observed, having in mind the quite large error in the determination. In a two state model B_2/B_1 is related to the differences of the molar volumes ΔV^0 and the compressibilities $\Delta\beta^0$ at ambient pressure [13,45]. The slope of the straight line describing the data is $-1.65 \pm 0.06\,\mathrm{GPa}^{-1}$ (Fig. 10). Surprisingly also the protons of the bases are located on the straight line describing the pressure dependence of chemical shifts. This indicates that the effect causing the pressure response of the chemical shifts is the same for the base protons and the ribose protons. A two states conformational equilibrium e. g. a *syn/anti* equilibrium could describe this behavior but other explanations are possible. According to Son and Chachaty [41] the *syn/anti* equilibrium is strongly correlated with the *N/S* equilibrium of the

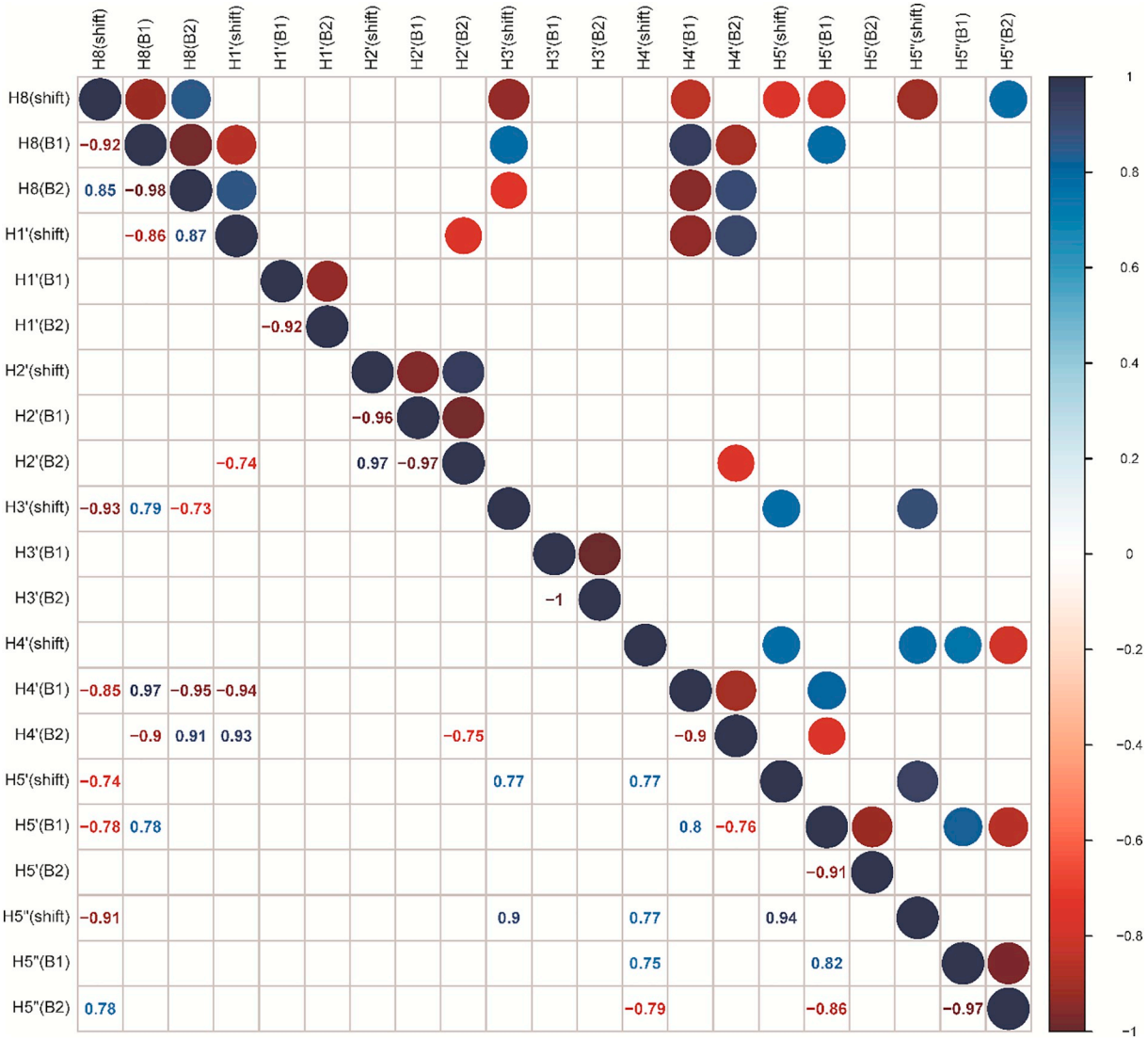

Fig. 8. Correlation between chemical shifts and first and second order pressure coefficients of guanine nucleotides in the absence and presence of $MgCl_2$.

ribose ring with the *anti*-conformation typical for the *N*-conformation of the ring [46,47]. In AMP and GMP the population of the *anti*-conformation is close to 100% according to Stolarski et al. [48]. In contrast, Guéron [49] reported a population of the *anti*-conformer of 70% for AMP and 47% for GMP, while according to Yathindra and Sundaralingam [50] these populations are of 92% form AMP and 0% for GMP. According to Imoto et al. [53], the population of the *anti*-conformer in AMP is 33%, of the *syn*-conformer between 25% and 43%, and 24% to 42% are in an intermediate state with a χ-angle between 60^0 and 130^0. Again a strong coupling of the N/S equilibrium is suggested with the *anti*-conformer in the *N*-conformation and the *syn*-conformer in the *S*-state [53]. However, this equilibrium is concentration dependent, in the stacked dimer the *anti/syn* as well as the coupled *N/S* equilibria are shifted towards the In addition, theoretical calculations performed on adenosine using force-field molecular dynamics (MD) or first-principles Car-Parrinello molecular dynamics (CPMD) showed a conformational equilibrium with fast *syn/anti* interconversion in water solvents [51].

Son and Chachaty [41] reported a population of the *anti*-conformer of 48% for ATP, 22% for ADP, and 0% for GTP, and 5% for GDP. The latter data do not agree with our ROE-patterns (Table 3). For a pressure induced population shift towards the *syn*-conformer, a downfield shift of the ribose H1′, H2′, as well as the H3′ resonances would be expected [48]. All three B_1-values are negative for AMP, ATP, GMP, GTP, and GTPγS. Provided the *syn-anti* transition is the responsible mechanism it would suggest a further increase of the *anti*-conformation with pressure. Only $GppCH_2p$ shows a downfield shift with pressure that may indicate a small increase of *syn*-conformation (Table 5). Nevertheless, the pressure effects on the H1′, H2′, as well as the H3′ are rather small compared to the expected shifts in the range of 0.11 to 0.72 ppm, meaning a possible shift of the equilibrium would also be rather small. The H4′ resonances show the largest pressure effects, the mean value of B_1 for adenine nucleotides and for guanine nucleotides is 0.098 and 0.116 ppm/GPa, respectively. If a shift of conformational equilibria is the main cause of the pressure effect then these data would suggest a change of the rotamer populations of the exocyclic methylene group.

The most extreme shift changes with pressure are observed for the H2 resonances in the Mg^{2+}-complexes of the adenine nucleotides. However, even the data points observed in these complexes are quite well described by an identical pressure dependence. It should be mentioned that the obtained ratio of B_2 to B_1 of $-1.65\,GPa\,mol^{-1}$ is also of similar magnitude as the values found for model peptides Ac-GGXA-NH_2, the mean ratio is -0.75 and $-0.8\,GPa\,mol^{-1}$ for the amide protons and amide nitrogens, respectively [45].

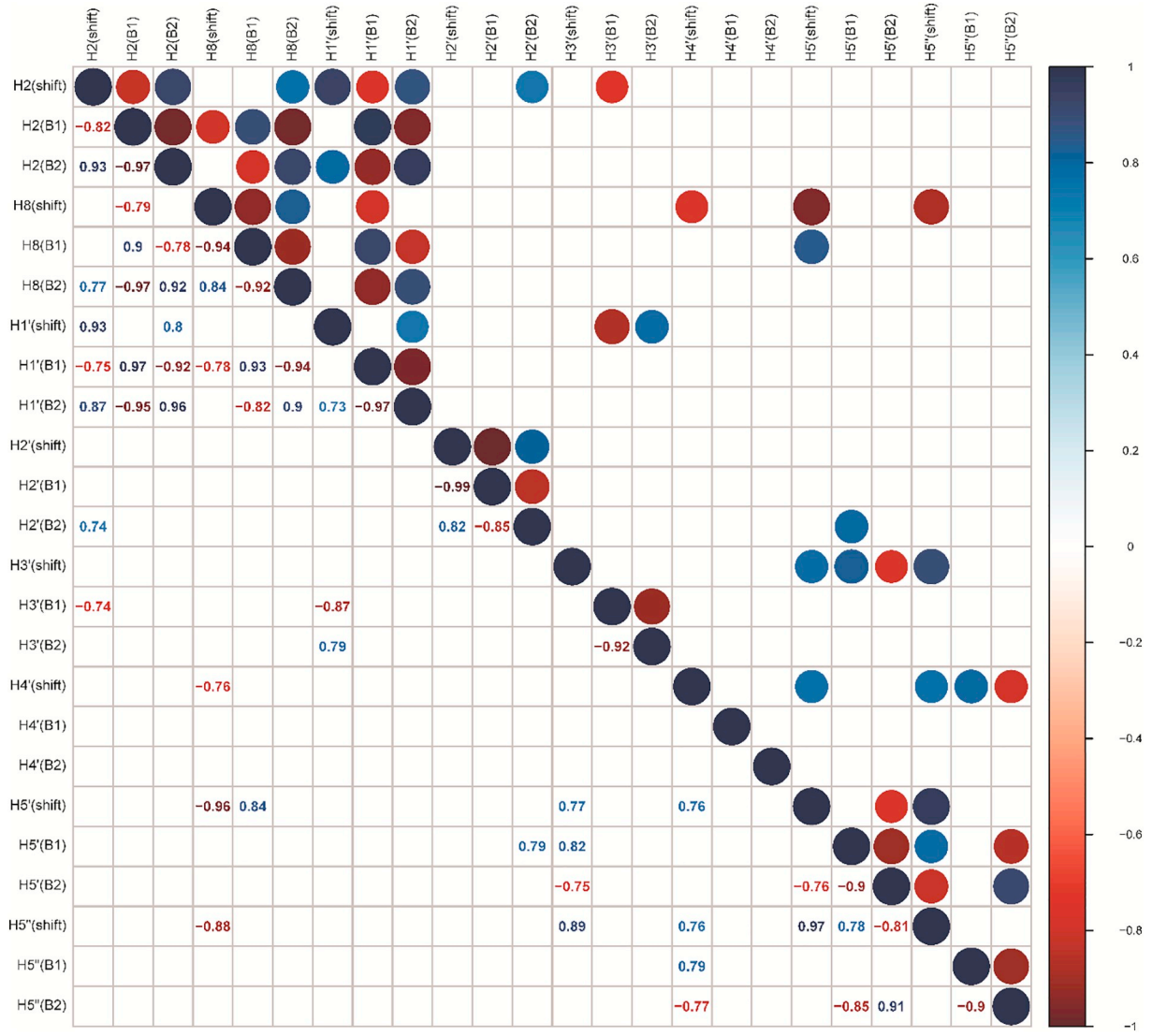

Fig. 9. Correlation between chemical shifts and first and second order pressure coefficients of adenine nucleotides in the absence and presence of $MgCl_2$.

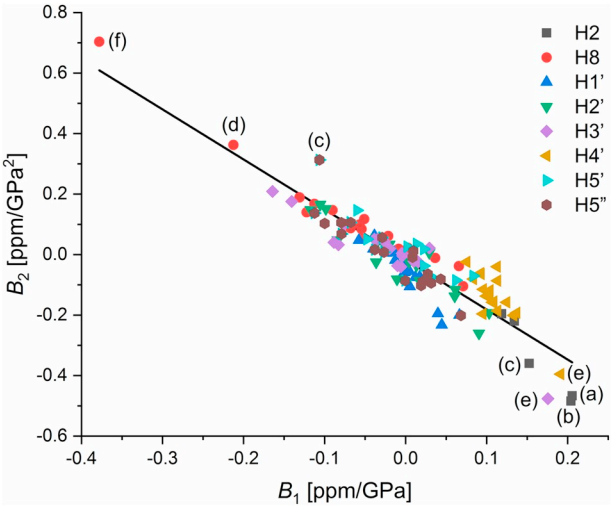

Fig. 10. Plot of the second order pressure coefficients B_2 versus B_1 for purine nucleotides. The slope B_2/B_1 is $-1.65 \pm 0.06\ GPa^{-1}$, the intercept -0.016 ± 0.005 ppm GPa^{-2}. Outliers are indicated that refer to (a) Mg^{2+}.ATP, (b) Mg^{2+}.ADP, (c) Mg^{2+}.AMP, (d) Mg^{2+}.GMP, (e) $GppCH_2p$, (f) Mg^{2+}.$GppCH_2p$.

5. Conclusion

The NMR assigments of the H5″ and H5′ protons reported in literature for purine nucleotides do not agree with our experimental data presented here, probably since they were just transferred from adenosine itself where they are correct but where the chemical shifts are inversed. The structural analyses in literature concerning the *syn-anti* equilibrium as well as the frequency of different ribose ring puckerings are contradictory. Here, we can present new data that solves these "historical" inconsistencies which may also partly be due to different experimental conditions in these studies (pH, ionic strength, temperature, nucleotide concentration). The quantum chemical calculations can give rather good values of chemical shifts but fail to predict the experimental equivalency of the H5″ and H5′ shifts in AMP. However, the frequency of the *N*- and *S* state of the ribose is well predicted. The data presented in this paper were mainly recorded for distinguishing more trivial pressure effects occurring in the free nucleotides and their Mg^{2+}-complexes from pressure effects that are due to the interaction with the protein and possible pressure induced conformational changes. In addition, the data presented here provide an experimental data base for testing future theoretical predictions that may elucidate the physical reason for the observed pressure dependent chemical shift changes that are not yet known in detail.

Acknowledgements

This work was funded by the Deutsche Forschungsgemeinschaft (DFG) under the Research Unit FOR 1979 (to H.R.K, W.K., S.M.K.) and under Germany's Excellence Strategy – EXC-233 – project number 390677874 (to S.M.K.), and by the Bayerische Forschungsstiftung (to H.R.K). We also thank the IT and Media Center (ITMC) of the TU Dortmund for computational support.

Appendix A. Supplementary data

Supplementary data to this article can be found online at https://doi.org/10.1016/j.bpc.2019.106261.

References

[1] K. Akasaka, H. Matsuki (Eds.), High Pressure Bioscience - Basic Concepts, Applications and Frontiers, Springer, Heidelberg, Germany, 2015.
[2] H. Le Chatelier, O. Boudouard, Limits of flammability of gaseous mixtures, Bull. Soc. Chim. Fr. 19 (1898) 483–488.
[3] T.Q. Luong, S. Kapoor, R. Winter, Pressure - a gateway to fundamental insights into protein solvation, dynamics, and function, ChemPhysChem 16 (2015) 3555–3571.
[4] H.R. Kalbitzer, I.C. Rosnizeck, C.E. Munte, P.N. Sunilkumar, V. Kropf, M. Spoerner, Intrinsic allosteric inhibition of signaling proteins by targeting rare interaction states detected by high pressure NMR spectroscopy, Angew. Chem. Int. Ed. 52 (2013) 14242–14246.
[5] H.R. Kalbitzer, M. Spoerner, P. Ganser, C. Hozsa, W. Kremer, A fundamental link between folding states and functional states of proteins, J. Am. Chem. Soc. 131 (2009) 16714–16719.
[6] M. Spoerner, M. Karl, P. Lopes, M. Hoering, K. Loeffel, A. Nuehs, J. Adelsberger, W. Kremer, H.R. Kalbitzer, High pressure 31P NMR on guanine nucleotides, J. Biomol. NMR 66 (2017) 141–157.
[7] M. Karl, M. Spoerner, T.-V. Pham, S.P. Narayanan, W. Kremer, H.R. Kalbitzer, Pressure response of 31P chemical shifts of adenine nucleotides, Biophys. Chem. 231 (2017) 50–54.
[8] H.R. Kalbitzer, A. Görler, H. Li, P.V. Dubovskii, W. Hengstenberg, C. Kowolik, H. Yamada, K. Akasaka, 15N and 1H NMR study of histidine containing protein (HPr) from Staphylococcus carnosus at high pressure, Protein Sci. 9 (2000) 693–703.
[9] J. Roche, J. Ying, A.S. Maltsev, A. Bax, Impact of hydrostatic pressure on an intrinsically disordered protein: A high-pressure NMR study of a-synuclein, ChemBioChem 14 (2013) 1754–1761.
[10] V. Tugarinov, D.S. Libich, V. Meyer, J. Roche, G.M. Clore, The energetics of a three-state protein folding system probed by high-pressure relaxation dispersion NMR spectroscopy, Angew. Chem. Int. Ed. 54 (2015) 11157–11161.
[11] G. Wagner, Activation volumes for the rotational motion of interior aromatic rings in globular proteins determined by high resolution 1H NMR at variable pressure, FEBS Lett. 112 (1980) 280–284.
[12] M. Hattori, H. Li, H. Yamada, K. Akasaka, W. Hengstenberg, W. Gronwald, H.R. Kalbitzer, Infrequent cavity-forming fluctuations in HPr from Staphylococcus carnosus revealed by pressure- and temperature-dependent tyrosine ring flips, Protein Sci. 13 (2004) 3104–3114.
[13] H.R. Kalbitzer, High pressure NMR methods for characterizing functional substates of proteins, in: K. Akasaka, H. Matsuki (Eds.), High Pressure Bioscience - Basic Concepts, Applications and Frontiers, Springer, Heidelberg, Germany, 2015, pp. 179–198.
[14] R. Frach, P. Kibies, S. Böttcher, T. Pongratz, S. Strohfeldt, S. Kurrmann, J. Koehler, M. Hofmann, W. Kremer, H.R. Kalbitzer, O. Reiser, D. Horinek, S.M. Kast, The chemical shift baseline for high pressure NMR spectra of proteins, Angew. Chem. Int. Ed. 55 (2016) 8757–8760.
[15] P. Wang, R.M. Izatt, J.L. Oscarson, S.E. Gillespie, 1H NMR study of protonation and Mg(II) coordination of AMP, ADP, and ATP at 25, 50, and 70 °C, J. Phys. Chem. 100 (1996) 9556–9560.
[16] H. Sigel, R. Griesser, Nucleoside 5′-triphosphates: self-association, acid-base, and metal ion binding properties in solution, Chem. Soc. Rev. 34 (2005) 875–900.
[17] M. Spoerner, A. Nuehs, P. Ganser, C. Herrmann, A. Wittinghofer, H.R. Kalbitzer, Conformational states of Ras complexed with the GTP analogue GppNHp or GppCH2p: implications for the interaction with effector proteins, Biochemistry 44 (2005) 2225–2236.
[18] M. Beck Erlach, C.E. Munte, W. Kremer, R. Hartl, D. Rochelt, D. Niesner, H.R. Kalbitzer, Ceramic cells for high pressure NMR spectroscopy of proteins, J. Magn. Reson. 204 (2010) 196–199.
[19] D.S. Raiford, C.G. Fisk, E.D. Becker, Calibration of methanol and ethylene glycol nuclear magnetic resonance thermometers, Anal. Chem. 51 (1979) 2050–2051.
[20] L. Braunschweiler, R.R. Ernst, Coherence transfer by isotropic mixing: Application to proton correlation spectroscopy, J. Magn. Reson. 61 (1983) 306–320.
[21] A. Bax, D.G. Davis, Practical aspects of two-dimensional transverse NOE spectroscopy, J. Magn. Reson. 63 (1985) 207–213.
[22] T.L. Hwang, A.J. Shaka, Cross relaxation without TOCSY: transverse rotating-frame Overhauser effect spectroscopy, J. Am. Chem. Soc. 114 (1992) 3157–3159.
[23] J.L. Markley, A. Bax, Y. Arata, C.W. Hilbers, R. Kaptein, B.D. Sykes, P.E. Wright, K. Wüthrich, Recommendations for the presentation of NMR structures of proteins and nucleic acids, Pure Appl. Chem. 70 (1998) 117–142.
[24] C.A.G. Haasnoot, F.A.A.M. de Leeuw, H.P.M. de Leeuw, C. Altona, Interpretation of vicinal proton-proton coupling constants by a generalized Karplus relation. Conformational analysis of the exocyclic C4′-C5′ bond in nucleosides and nucleotides, Recl. Trav. Chim. Pays-Bas 98 (1979) 576–577.
[25] C.A.G. Haasnoot, F.A.A.M. de Leeuw, C. Altona, The relationship between proton-proton NMR coupling constants and substituent electronegativities - I : an empirical generalization of the Karplus equation, Tetrahedron 36 (1980) 2783–2792.
[26] P.C. Kline, A.S. Serianni, Chiral hydroxymethyl groups: 1H NMR assignments of the prochiral C-5′ protons of ribonucleosides, Magn. Reson. Chem. 26 (1988) 120–123.
[27] N. Murali, Y. Lin, Y. Mechulam, P. Plateau, B.D. Rao, Adenosine conformations of nucleotides bound to methionyl tRNA synthetase by transferred nuclear Overhauser effect spectroscopy, Biophys. J. 72 (1997) 2275–2284.
[28] C.A.G. Haasnoot, F.A.A.M. de Leeuw, H.P.M. de Leeuw, C. Altona, The relationship between proton-proton NMR coupling constants and substituent electronegativities. II - conformational analysis of the sugar ring in nucleosides and nucleotides in solution using a generalized Karplus equation, Org. Magn. Reson. 15 (1981) 43–52.
[29] K. Inoue, H. Yamada, K. Akasaka, C. Herrmann, W. Kremer, T. Maurer, R. Döker, H.R. Kalbitzer, Pressure-induced local unfolding of the Ras binding domain of RalGDS, Nat. Struct. Biol. 7 (2000) 547–550.
[30] M.J. Frisch, G.W. Trucks, H.B. Schlegel, G.E. Scuseria, M.A. Robb, J.R. Cheeseman, G. Scalmani, V. Barone, B. Mennucci, G.A. Petersson, H. Nakatsuji, M. Caricato, X. Li, H.P. Hratchian, A.F. Izmaylov, J. Bloino, G. Zheng, J.L. Sonnenberg, M. Hada, M. Ehara, K. Toyota, R. Fukuda, J. Hasegawa, M. Ishida, T. Nakajima, Y. Honda, O. Kitao, H. Nakai, T. Vreven, J.A. Montgomery Jr., J.E. Peralta, F. Ogliaro, M. Bearpark, J.J. Heyd, E. Brothers, K.N. Kudin, V.N. Staroverov, R. Kobayashi, J. Normand, K. Raghavachari, A. Rendell, J.C. Burant, S.S. Iyengar, J. Tomasi, M. Cossi, N. Rega, J.M. Millam, M. Klene, J.E. Knox, J.B. Cross, V. Bakken, C. Adamo, J. Jaramillo, R. Gomperts, R.E. Stratmann, O. Yazyev, A.J. Austin, R. Cammi, C. Pomelli, J.W. Ochterski, R.L. Martin, K. Morokuma, V.G. Zakrzewski, G.A. Voth, P. Salvador, J.J. Dannenberg, S. Dapprich, A.D. Daniels, Ö. Farkas, J.B. Foresman, J.V. Ortiz, J. Cioslowski, D.J. Fox, Gaussian 09, Revision E.01, Gaussian, Inc., Wallingford CT, 2009.
[31] T. Kloss, J. Heil, S.M. Kast, Quantum chemistry in solution by combining 3D integral equation theory with a cluster embedding approach, J. Phys. Chem. B 112 (2008) 4337–4343.
[32] S.M. Kast, T. Kloss, Closed-form expressions of the chemical potential for integral equation closures with certain bridge functions, J. Chem. Phys. 129 (2008) 236101.
[33] J. Wang, R.M. Wolf, J.W. Caldwell, P.A. Kollman, D.A. Case, Development and testing of a general amber force field, J. Comput. Chem. 25 (2004) 1157–1174.
[34] J. Wang, W. Wang, P.A. Kollman, D.A. Case, Automatic atom type and bond type perception in molecular mechanical calculations, J. Mol. Graph. Model. 25 (2006) 247–260.
[35] N. Tielker, D. Tomazic, J. Heil, T. Kloss, S. Ehrhart, S. Güssregen, K. Friedemann Schmidt, The SAMPL5 challenge for embedded-cluster integral equation theory: solvation free energies, aqueous pK_a, and cyclohexane-water log D, J. Comput. Aided Mol. Des. 30 (2016) 1035.
[36] N. Tielker, L. Eberlein, S. Güssregen, S.M. Kast, The SAMPL6 challenge on predicting aqueous pK_a values from EC-RISM theory, J. Comput. Aided Mol. Des. 32 (2018) 1151.
[37] R. Frach, S.M. Kast, Solvation effects on chemical shifts by embedded cluster integral equation theory, J. Phys. Chem. A 118 (2014) 11620–11628.
[38] M.J. Frisch, G.W. Trucks, H.B. Schlegel, G.E. Scuseria, M.A. Robb, J.R. Cheeseman, G. Scalmani, V. Barone, G.A. Petersson, H. Nakatsuji, X. Li, M. Caricato, A.V. Marenich, J. Bloino, B.G. Janesko, R. Gomperts, B. Mennucci, H.P. Hratchian, J.V. Ortiz, A.F. Izmaylov, J.L. Sonnenberg, D. Williams-Young, F. Ding, F. Lipparini, F. Egidi, J. Goings, B. Peng, A. Petrone, T. Henderson, D. Ranasinghe, V.G. Zakrzewski, J. Gao, N. Rega, G. Zheng, W. Liang, M. Hada, M. Ehara, K. Toyota, R. Fukuda, J. Hasegawa, M. Ishida, T. Nakajima, Y. Honda, O. Kitao, H. Nakai, T. Vreven, K. Throssell, J.A. Montgomery Jr., J.E. Peralta, F. Ogliaro, M.J. Bearpark, J.J. Heyd, E.N. Brothers, K.N. Kudin, V.N. Staroverov, T.A. Keith, R. Kobayashi, J. Normand, K. Raghavachari, A.P. Rendell, J.C. Burant, S.S. Iyengar, J. Tomasi, M. Cossi, J.M. Millam, M. Klene, C. Adamo, R. Cammi, J.W. Ochterski, R.L. Martin, K. Morokuma, O. Farkas, J.B. Foresman, D.J. Fox, Gaussian 16, Revision B.01, Gaussian, Inc., Wallingford CT, 2016.
[39] P.C. Bevilacqua, T.S. Brown, S. Nakano, R. Yajima, Catalytic roles for proton transfer and protonation in ribozymes, Biopolymers 73 (2004) 90–109.
[40] H. Rosemeyer, G. Tóth, B. Golankiewicz, Z. Kazimierczuk, W. Bourgeois, U. Kretschmer, H.P. Muth, F. Seela, Syn-anti conformational analysis of regular and modified nucleosides by 1D 1H NOE difference spectroscopy: a simple graphical method based on conformationally rigid molecules, J. Organomet. Chem. 55 (1990) 5784–5790.
[41] T.-D. Son, C. Chachaty, Proton NMR and spin lattice relaxation study of nucleosides di- and triphosphates in neutral aqueous solution, Biochim. Biophys. A. 500 (1977) 405–418.
[42] C. Giessner-Prettre, B. Pullman, Quantum mechanical calculations of P-C and P-H spin-spin coupling constants in model compounds and in nucleotides, J. Theor. Biol. 48 (1974) 425–443.
[43] D.B. Davies, S.S. Danyluk, Nuclear magnetic resonance studies of 5′-ribo- and deoxyribonucleotide structures in solution, Biochemistry 13 (1974) 4417–4434.
[44] B.J. Blackburn, R.D. Lapper, I.C.O. Smith, A proton magnetic resonance study of the conformations of 3′5′-cyclic nucleotides, J. Am. Chem. Soc. 95 (1973) 2873–2878.
[45] M. Beck Erlach, J. Koehler, B. Moeser, D. Horinek, W. Kremer, H.R. Kalbitzer, Relationship between non-linear pressure induced chemical shift changes and thermodynamic parameters, J. Chem. Phys. B 18 (2014) 5681–5690.

[46] M. Sundaralingam, Stereochemistry of nucleic acids and their constituents.† IV. Allowed and preferred conformations of nucleosides, nucleoside mono-, di-, tri-, tetraphosphates, nucleic acids and polynucleotides, Biopolymers 7 (1969) 821–860.
[47] H.-D. Lüdemann, E. Westhof, O. Röder, A dynamic correlation between ribose conformation and glycosyl torsion angle of dissolved xanthosine studied by continuous-wave-mode and pulsed nuclear-magnetic-resonance methods, Eur. J. Biochem. 49 (1974) 143–150.
[48] R. Stolarski, L. Dudycs, D. Shugar, NMR studies of the syn-anti dynamic equilibrium in purin nucleosides and nucleotides, Eur. J. Biochem. 108 (1980) 111–121.
[49] M. Guéron, C. Chachaty, T.-D. Son, Properties of purine nucleotides studied by the Overhauser effect: conformations, flexibility, aggregation, Ann. N. Y. Acad. Sci. 222 (1973) 307–323.
[50] N. Yathindra, M. Sundaralingam, Conformational studies on guanosine nucleotides and polynucleotides. The effect of the base on the glycosyl and backbone conformations, Biopo*lymers* 12 (1973) 2075–2082.
[51] N.A. Murugan, H.W. Hugosson, Solvent dependence of conformational distribution, molecular geometry, and electronic structure in adenosine, J. Phys. Chem. B 113 (2009) 1012–1021.
[52] F.E. Evans, R.H. Sarma, Intermolecular orientations of adenosine-5′- monophosphate in aqueous solution as studied by fast fourier transform ‘H NMR spectroscopy, Biopolymers 13 (1974) 2117–2132.
[53] T. Imoto, S. Shibata, K. Akasaka, H. Hatano, Conformation of adenosine 5′-monophosphate in aqueous solution as studied by NMR-DESERT method, Biopolymers 16 (1977) 2705–2721.
[54] T. Pongratz, P. Kibies, L. Eberlein, N. Tielker, C. Hölzl, S. Imoto, M. Beck, Erlach, S. Kurrmann, P.H. Schummel, M. Hofmann, O. Reiser, R. Winter, W. Kremer, H.R. Kalbitzer, D. Marx, D. Horinek, S.M. Kast, Pressure-dependant electronic structure calculation using integral equation based solvation models, Biophys. Chem. (2019), https://doi.org/10.1016/j.bpc.2019.106258.